Development of a methodology for the characterisation of native graphite in a gold ore by an automated mineralogy system

Auteur : Lenoir, Laura
Promoteur(s) : Pirard, Eric
Faculté : Faculté des Sciences appliquées
Diplôme : Master en ingénieur civil des mines et géologue, à finalité spécialisée en ressources minérales et recyclage
Année académique : 2022-2023
URI/URL : http://hdl.handle.net/2268.2/18153

University of Liège

Faculty of Applied Sciences

Development of a methodology for the characterisation of native graphite in a gold ore by an automated mineralogy system

Master's Thesis completed by

Laura Lenoir

in order to obtain the degree of Master in Mining and Geological Engineering

Academic supervisor: Eric PIRARD

Jury: Hassan BOUZAHZAH,

Frédéric HATERT,

Raphaël MERMILLOD-BLONDIN

Academic Year: 2022-2023

Abstract

When a gold deposit contains carbonaceous material such as graphite, the processing plant may face a loss in the gold recovery because of the preg-robbing generated. The preg-robbing capacity of the carbonaceous material, and therefore the associated gold loss, depends on several parameters such as the surface and the crystallinity/maturity of the carbonaceous material, but also on the organic matter content, as well as the presence of different functional groups on the surface of the carbon material. Thus, it is necessary to be able to characterise it.

This thesis focuses on a technique of characterisation of graphite (carbonaceous material) by an automated mineralogy system based on a scanning electron microscope that allows to evaluate the liberation and associations of minerals and to quantify them. To do this, samples must be mounted in polished blocks, however, the usual preparation, which consists of a homogeneous mixture of epoxy resin, hardener and an aliquot of material, poses several problems such as differential sedimentation of the particles, touching particles and systematic orientation of the particles. In addition, the backscattered electron image of the scanning electron microscope shows a low contrast between graphite and epoxy resin due to their similar average atomic number. Tests had been done in the past at the University of Liège to solve this issue but were inconclusive. The main objective of this thesis was to develop a polished block preparation that allowed the native graphite of a gold deposit to be analysed via a scanning electron microscope. A series of tests based on the preparation usually used at the University of Liège and on the information found in the literature review was conducted. The results of the various tests carried out made it possible to establish a polished block preparation allowing the characterisation of the native graphite by an automated mineralogy system based on a scanning electron microscope although additional work on the method of polishing is necessary.

Résumé

Lorsqu'un gisement d'or contient de la matière carbonée tel que du graphite, l'usine de traitement peut faire face à une perte dans la récupération de l'or à cause du preg-robbing engendré. La capacité de preg-robbing de la matière carbonée, et donc la perte en or associée, dépend de plusieurs paramètres tels que la surface et la cristallinité/maturité de la matière carbonée, mais aussi de la teneur en matière organique, ainsi que la présence de différents groupements fonctionnels à la surface de la matière carbonée. Ainsi, il est nécessaire de pouvoir la caractériser.

Cette thèse se porte sur une technique de caractérisation du graphite (matière carbonée) par un système de minéralogie automatisé basé sur un microscope électronique à balayage qui permet d'évaluer la libération et les associations des minéraux ainsi que de les quantifier. Pour se faire, les échantillons doivent être montés en section polie, cependant, la préparation habituelle, qui consiste en un mélange homogène de résine époxy, de durcisseur et d'une aliquote de matière, pose plusieurs problèmes tels que la sédimentation différentielle des particules, le contact des particules entre elles et l'orientation systématique des particules. De plus, l'image en électrons rétrodiffusés du microscope électronique à balayage montre un faible contraste entre le graphite et la résine époxy en raison de leur numéro atomique moyen similaire. Des tests avaient été effectués par le passé à l'Université de Liège pour résoudre ce problème mais n'avaient pas été inconcluant. L'objectif principal de cette thèse était de développer une préparation de section polie qui permettait d'analyser le graphite natif d'un gisement d'or via un microscope électronique à balayage. Une série de tests basés sur la préparation habituellement utilisée à l'Université de Liège et sur les informations trouvées dans la revue de littérature a été réalisée. Les résultats des différents tests ont permis d'établir une préparation de section polie permettant la caractérisation du graphite natif par un système de minéralogie automatisé basé sur un microscope électronique à balayage bien qu'un travail supplémentaire sur la méthode de polissage soit nécessaire.

Acknowledgements

I would like to thank my supervisor, Prof. Dr. Eric Pirard, for allowing me to carry out this project and who through a small course in bachelor made me discover the world of geology. Through this, I would also like to thank all my teachers who have allowed me to advance in my life and who have allowed me to shape my person through learning.

I am especially grateful to my co-supervisor, Hassan Bouzahzah, for his availability, guidance, and interest throughout this work. I thank him for his kindness and for the long hours of explanations about the different topics related to this work.

I would also like to thank Raphaël Mermillod-Blondin, without whom my internship would not have been possible. I thank him for his involvement and interest in the subject and I am thankful for the hospitality and support from people on the site.

More personally, I would like to thank my parents, my brother and all my family for their support and encouragement. Thank you, Alexandre, for being a caring and loving big brother, who often helps me clear my mind. I'm also grateful to all my friends for the joy they bring me and the friendship they offer me. I would especially like to thank my partner, Arthur, who has given me motivation and support from the beginning. Thank you for your love even in my lowest moments.

Table of Contents

Table of Figures

List of Tables

1 Introduction

Gold is a precious metal with a high economic value. It is durable, malleable, ductile and a good conductor of heat and electricity. As a result, it is used in electronic devices, as well as in other applications such as jewellery and ornaments.

Its concentration in the earth crust is around 0.005 ppm (Marsden & House, 2006). It can occur as an element or as a natural alloy with silver (electrum), or be bound to other minerals such as sulphur, arsenic, tellurium, antimony, and selenium.

There are different types of process for recovering gold, such as gravity separation, flotation, leaching (e.g., cyanidation or other alternative leaching processes) and amalgamation. Depending on the ore, it may first require refractory treatment to release encapsulated gold. Among the different processes, cyanidation, which is often followed by carbon adsorption or by zinc precipitation for gold recovery, is nowadays the most common one.

However, cyanidation raises a certain number of concerns. In addition to the environmental impact, gold dissolution can lead to significant losses due to the presence of carbonaceous material, a phenomenon known as preg-robbing.

1.1 Preg-robbing

Pre-robbing is the phenomenon whereby gold in soluble form, such as gold cyanide complex, is captured by ore constituents in the same way that the complex is adsorbed and recovered by activated carbon, for example, in carbon-in-leach (CIL) circuit. These constituents include carbonaceous materials and the minerals themselves, such as sulphides and certain types of clays and silicates. The mechanisms of capture include: adsorption, reduction on the mineral surface, and absorption (Rees & Van Deventer, 2000; Goodall *et al.*, 2005; Ng *et al.*, 2022). The paper of Ng *et al.* (2022) provided a good summary of the state of the art concerning preg-robbing.

The authors tend to agree that carbonaceous material shows a greater adsorption capacity, of which native carbon would be the most preg-robbing material. This is why the rest of this literature review focuses on the different types of carbonaceous material.

1.1.1 Carbonaceous material (CM)

Studies on Carlin ore by Radtke & Scheiner (1970) showed two types of carbonaceous compounds in addition to activated carbon material (native carbon): a mixture of heavy hydrocarbons which would coat the surfaces of the activated carbon material and, an organic acid, similar to humic acid. Studies by Osseo-Asare *et al.* (1984) also determined these three categories of carbonaceous materials, i.e., heavy hydrocarbons, organic acids, and natural/elemental carbon. The study by Pyke *et al.* (1999) showed that carbonates have little effect on preg-robbing.

Hydrocarbons do not interact with gold and have been found to enhance gold recovery due to their coating around the native carbon, which decreases the surface area available to adsorb gold onto

native carbon (main preg-robber) and therefore decreases preg-robbing (Radtke & Scheiner, 1970; Guay, 1981; Osseo-Asare *et al.*, 1984). Although in the case of the Pyke *et al.* study (1999), the improvement in recovery was minimal and within experimental error.

Humic substances, such as humic acid, increase gold losses by adsorbing it or complexing it to a stable compound under oxidising conditions. However, it has been shown in the study of Stenebråten *et al.* (1999) that these substances, if any in the ore, do not have a great influence on the preg-robbing. In the case of the study of Pyke *et al.* (1999), humic acid has a negligible effect on gold recovery and thus on preg-robbing. On the other hand, when the ore has no carbonaceous material and humic acid is added, as in the study by Van den Berg (2000), significant gold losses were observed.

Finally, studies by Osseo-Asare *et al.* (1984) and Pyke *et al.* (1999) have shown that native carbon has the highest capacity to adsorb gold, although this capacity is lower than that of activated carbon. This statement seems to be the general consensus among the authors (Ng *et al.*, 2022).

1.1.2 Adsorption capacity of CM

Different factors have been proposed for the determination of preg-robbing capacity.

It seems that the adsorption capacity has some correlation with the thermal maturity of the carbon. Indeed, the research by Van Vuuren *et al.* (2000) showed that peat, lignite, semi-anthracite, and anthracite had the highest gold adsorption values, of which the latter had the highest. Between the two groups (peat – lignite, and semi-anthracite - anthracite) the values decreased. Medium volatile bituminous coals had the lowest one. On another hand, Ofori-Sarpong *et al.* (2010) studied biotreatment to reduce preg-robbing capacity on four types of coal : lignite, subbituminous, bituminous and anthracite. Before the application of the treatment, the first three had similar adsorption capacity while anthracite had the highest capacity. It would seem that the greater the thermal maturity of the carbon is, the more it is preg-robbing.

Moreover, Stenebråten *et al.* (2000) demonstrated that the absorption capacity of Goldstrike ore was inversely proportional to the crystallite size Lc (002) calculated from XRD analysis. Indeed, the larger the crystallites are, the smaller the preg-robbing is and the more mature the carbon is (from amorphous activated carbon to crystalline graphite). They speculated that the high adsorption of the smaller crystallites was due to irregularities in their edges. Actually, their larger d-spacing is supposed to enable the appearance of defects and irregularities in the crystallite edge.

This leads to the definition of disorder in the crystal lattice. The degree of disorder refers to: “structural deviations from the well-defined three-dimensional structure of crystalline graphite of the carbonaceous material” (Helm *et al.,* 2009). Raman spectroscopy is a non-destructive tool that allows characterising the degree of disorder in CM, and thus their type. In the spectrum, properly crystallised graphite samples show a single dominant G band, while any deviation from this structure results in the broadening of the G band (around 1580-1600 cm^{-1}) and the development of a D band (around 1330-1550 cm^{-1}) (Helm *et al.,* 2009; Hart *et al.*, 2011). Helm *et al.* (2009) studied the correlation between preg-robbing and Raman spectroscopy. They observed a positive correlation between their ratio calculated using the height and width of the D and G bands, and their preg-robbing value. As a result, the graphitic carbon that generated high preg-robbing has Raman spectra similar to those of activated carbon (which has a higher degree of disorder), while the graphitic carbon inducing low preg-robbing has spectra similar to those of natural graphite.

Another factor identified in the work by Stenebråten *et al.* (2000) shows that the preg-robbing behaviour of the CM usually increases with increasing surface area. In the same study, they also noted an inverse correlation between gold adsorption and pore size, such that a smaller pore diameter exhibits a greater adsorption capacity.

1.2 Characterisation of CM

The preg-robbing capacity of carbonaceous material therefore depends on various parameters as surface area and crystallinity (/maturity), but also the organic matter content (also known as total organic carbon: TOC), as well as the presence of various functional groups on the surface of the CM (Dimov & Hart, 2016).

1.2.1 TOC

Analysis of organic carbon content can be carried out using chemical assays. However, it is necessary to eliminate inorganic carbon (total inorganic carbon: TIC). These two variables are linked to the total carbon value (TC) as follows:

$$TC = TOC + TIC$$

This is usually done by treating the sample with non-oxidising acids such as H_2SO_4 and HCl, which release CO_2 and H_2O. The most commonly used method for rock samples is the dry method, which involves complete combustion of the sample in a carbon-free atmosphere. The intensity of the CO_2 peak released is then quantified by a non-dispersive infrared detection cell. A combustion analyser, such as the LECO analyser, could be used to fulfil these roles (Raja & Barron, 2023).

1.2.2 Crystallinity/maturity

Maturity, which is defined here as its proximity to activated carbon or well-crystallised graphite, as for the degree of disorder, could be estimated through Raman spectrometry. Indeed, the spectrum of the native carbon is placed in respect to the spectra of activated carbon and well-crystallised graphite. A (native) carbon with a spectrum closer to activated carbon would imply a greater preg-robbing capacity.

1.2.3 Surface area

The native carbon available surface area depends on three parameters: its size, its porosity and its liberation. The size of native carbon particle could be analysed with, for example, the use of sieves. Its porosity can be assessed with a BET surface analysis. Its liberation - and by extension, its associations – can be analysed with, for instance, an optical microscope or a Scanning Electron Microscope (SEM).

For the latter two, samples – ground or not - are mounted in polished blocks as they represent the support necessary for the observation of the sample under the microscope (optical and electronic) and for the acquisition of digital images that will be used for image analysis and mineralogical quantification (with the SEM). However, the usual preparation, which consists of a homogeneous mixture of epoxy resin, hardener and a spoonful of material, poses several problems such as differential sedimentation

of the particles, touching particles and systematic orientation of the particles (Jackson *et al.*, 1984). In addition, the Scanning Electron Microscope Backscattered Electron image shows a low contrast between the organic matter and the epoxy resin due to their similar average atomic number (Rahfeld & Gutzmer, 2017) as seen in Figure 1.

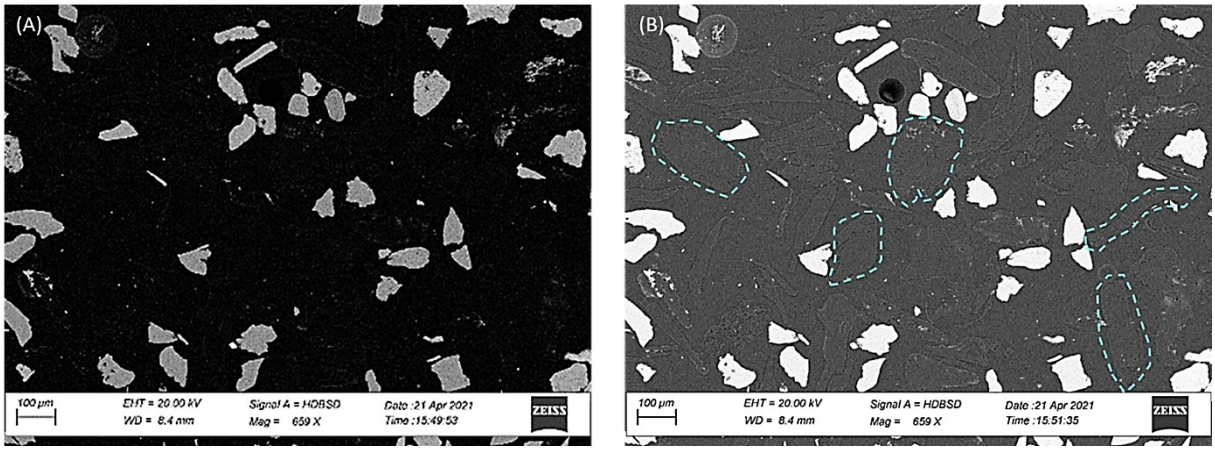

Figure 1: on the left (A), figure with proper brightness shows the low contrast between epoxy resin and graphite under the SEM; on the right (B), same figure with light overexposure. The dotted blue line shows the contour of some graphite particles in the polished block that could not be seen with proper brightness

1.3 Objectives of the thesis

This work focuses on one of the methods for characterising carbonaceous material, namely the Scanning Electron Microscope. The aim of this work is therefore to develop a preparation of polished blocks allowing a good characterisation of carbonaceous material, and more particularly graphite in this case, by solving the problems encountered in the traditional preparation method and creating a good contrast between the resin and the graphite. This work is a continuation of tests previously carried out at the University of Liège. These tests were unfortunately inconclusive as explained in a following section (Chapter 3: Polished blocks at ULiège).

To achieve these objectives, a literature review on the preparation of polished blocks (**Chapter 2**), followed by how blocks are usually prepared at the University of Liège with a detail on tests already carried out on this issue (**Chapter 3**) will be conducted to determine the best course of action which will be detailed in the following chapter “Material and methods” (**Chapter 4**). As its name indicates, this chapter will present the samples to be characterised with the final preparation, as well as a series of actions (tests) to be carried out to determine the preparation that will best meet the objectives (=final preparation). It is in the following chapter, “Results and discussion” (**Chapter 5**) that will be presented and interpreted the results of the tests as well as the validation of the preparation by the characterisation of the samples under the SEM.

2 State of the art: Polished block preparation

2.1 Traditional polished block preparation for automated mineralogy system

Traditional polished block (PB) preparation consists of a homogeneous mixture of epoxy resin, hardener and an aliquot of material (particles) in a 25 or 30mm diameter mould (Jackson *et al.*, 1984; Sylvester 2012; Grant *et al.*, 2016; Donskoi *et al.*, 2018). This is usually followed by the use of a vacuum chamber which allows the particles to be completely impregnated into the resin and the minimization of air bubbles. Then, as some authors proposed, the mould could be transferred to a pressure vessel or curing oven for the resin to be fully cured (Sandmann, 2015; Donskoi *et al.*, 2018).

However, Jackson *et al.* (1984) identified possible sources of error associated with the preparation of polished blocks that could affect the results of an automated mineralogical analysis. Among them are:

- Differential particles sedimentation (segregation), either by density segregation between particles of different modal mineralogy (different density), or either by segregation between small (lighter) and large (heavier) particles, especially for unsized samples. Thus, heavier minerals will dominate the surface of the sample and therefore the amount of heavy minerals will be overestimated.
- Touching particles which will be interpreted as a single particle by the automated mineralogy software influencing the liberation and association analysis and causing erroneous results.
- Systematic particle orientation which may induce biased measurements in terms of size and shape.

Jackson *et al.* (1984) then proposed a method for preparing polished blocks that would limit these errors. As a first step, it is suggested to use calibrated (sized) samples to minimize segregation caused by differences in particle size. Then, a sample-graphite mix (in the same size range as the sample) is recommended to avoid segregation and particles in contact where the ratios proposed depend on the sample size. However, Kwitko-Ribeiro (2012), revealed that for this sample-graphite mixture, there is strong mineral segregation. In the resin, the graphite tends to float and separate from the sinking sample. Moreover, the results of Røisi & Aasly's (2018) study suggests that using graphite as a filler does not necessarily prevent segregation, at least if the epoxy resin-graphite-sample ratio is not taken into account. They went on to suggest that vertical sections should be used for most mineral liberation and modal mineralogy studies to ensure that results are not biased by segregation.

As the sedimentation of the particles persists, other authors have proposed procedures to minimize this sedimentation. As suggested above by Røisi & Aasly (2018) but also proposed by other authors, a method widely used to avoid carrying out biased analyses due to sedimentation is to use vertical sections (also called transverse sections or cross sections). The section is moulded a first time then it is cut along its length and moulded again as seen in Figure 2. Although this procedure takes more time and material, it is supposed to better represent the sample by allowing the entire sedimentation area to be analysed (Hiemstra, 1985; Shaffer, 2009; Butcher, 2010; Smythe *et al.*, 2013; Sandmann, 2015; Grant *et al.*, 2016; Røisi & Aasly, 2018). In this regard, Grant *et al.* (2016) proposed a single-step trans-vertical epoxy preparation method which would reduce the working time and would even be more economical than a traditional round mould, but it requires custom-made equipment.

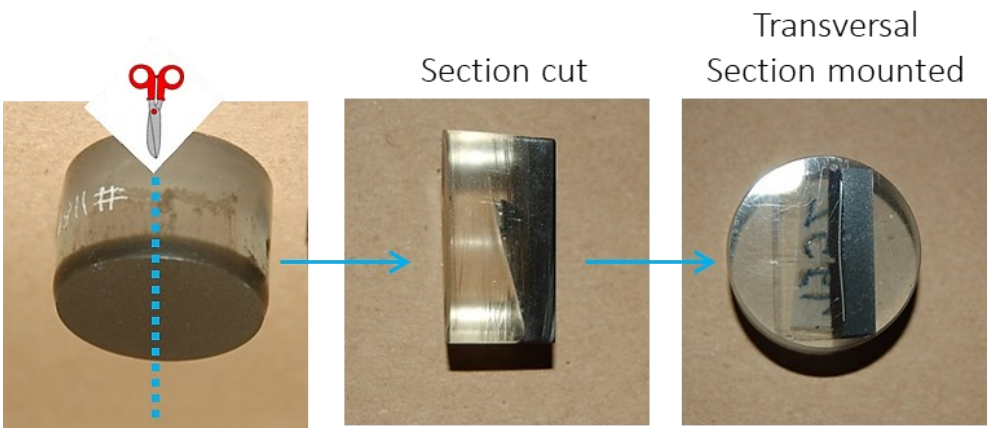

Figure 2: Vertical section production steps (modified from Bouzahzah, 2013)

Another method proposed by Kwitko-Ribeiro (2012), suggested inducing slow rotational motion during curing time (dynamic curing sample preparation process as seen in Figure 3).

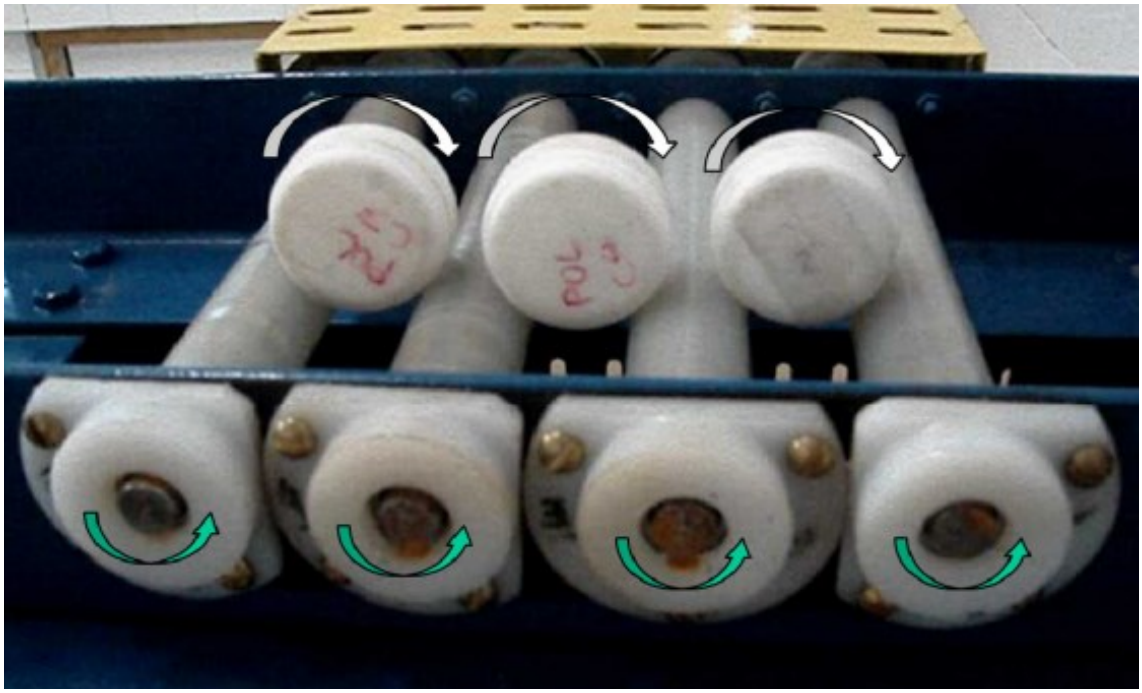

Figure 3 : Device for dynamic curing by rolling of 30 mm diameter moulds (from Kwitko-Ribeiro, 2012)

Sandmann (2015) proposes a flowchart modified from the Field Electron and Ion Company (FEI company) which suggests which type of preparation method to use depending on the type of material (granular or not), whether it is calibrated or not (unsized or sized), whether the size of the sample is rather coarse, in which case the addition of graphite is not recommended, and if some sedimentation is expected, in which case it is advisable to make a vertical section.

In the same line of thought, to overcome the recurrent problems of the traditional preparation, Bouzahzah *et al.* (2015) have proposed another way of preparing polished blocks. As for the other methods, the powdered sample is prepared by means of an inclusion in an epoxy resin which forms a matrix for observation and grain analysis. The innovation comes from the addition of nano black carbon particles to this mixture. In fact, per section, they mentioned that 0.4 g of black carbon is mixed with 16.5 g of resin (EpoFix Resin by Struers). Afterwards, this mixture is homogenised using a mechanical stirrer and a slightly inclined four-bladed propeller (Figure 4). They indicated that the mixing is done at

300 rpm for 3 hours. The preparation is then degassed overnight under vacuum. The next day, the hardener can be added, i.e., two grams of hardener per section are poured into the resin and mixed for a few minutes. Finally, the resin is added to a small spoonful of sample (about 1g) in a plastic mould. This is mixed homogeneously for a few minutes and left overnight to harden. Polishing can begin the next day after removal from the mould. It was explained that black carbon is used to prevent sedimentation of the grains and to obtain an excellent spatial dispersion of those grains. In addition, the addition of 0.4g of BC for 16.5g of resin makes it conductive, which prevents the accumulation of electronic charges on the surface of the polished block studied under the electron microscope (SEM). However, this conductivity is only found for particles smaller than 100 µm.

Figure 4: Mechanical stirrer and slightly inclined four-bladed propeller.

2.2 Low contrast between solid organic matter and epoxy resin

As mentioned, epoxy resins are the main embedding media for polished blocks. Their main advantages are good preservation of ultrastructures, little to no shrinkage, the easiness of sectioning and a decent degree of stability in the electron beam (Mollenhauer, 1993). However, the BSE image shows no contrast between organic matter and epoxy resin due to their similar average atomic number. In these cases, such as analyses on organic coal particles, carnauba wax or a halogenated epoxy resin is generally used when observing this type of material under SEM with the Backscattered Electron observation mode (O'Brien *et al.*, 2011; Rahfeld & Gutzmer, 2017).

Regarding the use of halogenated resin, Gomez *et al.* (1984) showed that EDX signals of brominated epoxy resin display an interference of bromine (Br) and aluminium (Al). Therefore, it was not considered suitable. Creelman & Ward (1996) used an epoxy resin which was composed of chlorinated material. However, the BSE image of this resin was similar (grayscale) to that of their organic matter. Thus, they added iodoform to their resin which was found to provide a better contrast.

The study of Rahfeld & Gutzmer (2017) compared the use of iodized resin and carnauba wax as an impregnation material. It was determined that the best results were obtained with an iodized resin containing 15% by weight of iodoform and that carnauba wax did not prove to give sufficient contrast compared to the organic matter of their ore (Kupferschiefer).

3 Polished blocks at ULiège

The University of Liège (ULiège) has a SEM based automated mineralogy system used for all kinds of projects. Indeed, automated mineralogy based on SEM allows the analysis of a large number of mineral grains to represent the sample as accurately as possible and to generate particle-specific data for the subsequent interpretation. Ground samples are therefore usually mounted in polished blocks using the method proposed by Bouzahzah *et al.* (2015).

Many current projects require the characterisation of graphite, either for primary or secondary ore (e.g., battery recycling). For this purpose, a number of tests were carried out based on the method currently used at ULiège (Bouzahzah *et al.*, 2015), with the addition of iodoform ("Iodoform, 99%" of Thermo Scientific Chemicals) to create a good contrast between the resin and the graphite, as proposed by Rahfeld & Gutzmer (2017). The Bouzahzah *et al.* (2015) method is estimated to be the best preparation for polished blocks currently available since the black carbon used is a powder of carbon nanoparticles not visible under the SEM. Indeed, the addition of graphite to the resin as proposed by certain authors is not conceivable to avoid sedimentation because the aim is to be able to characterize the graphite of the ore.

However, it was noticed that an exothermic reaction took place when the whole (resin - hardener - black carbon - iodoform - sample) was mixed resulting in cracks and large bubbles in the resin block (Figure 5) which are not welcome for two reasons. Firstly, the grey level of the resin is similar to that of native carbon (see Figure 6) making the SEM-AM waste time analysing it, and secondly, making the analyses biased due to the same grey level.

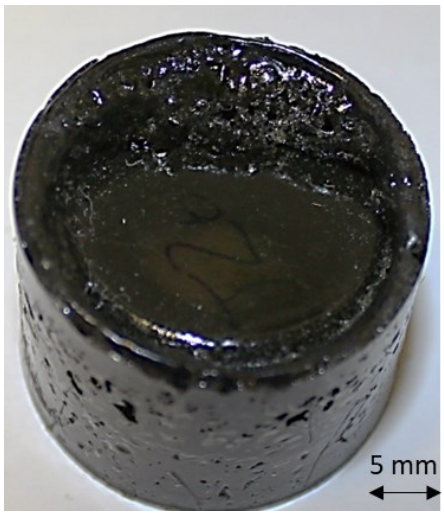

Figure 5: Result of a previous test showing the exothermic reaction that occurred

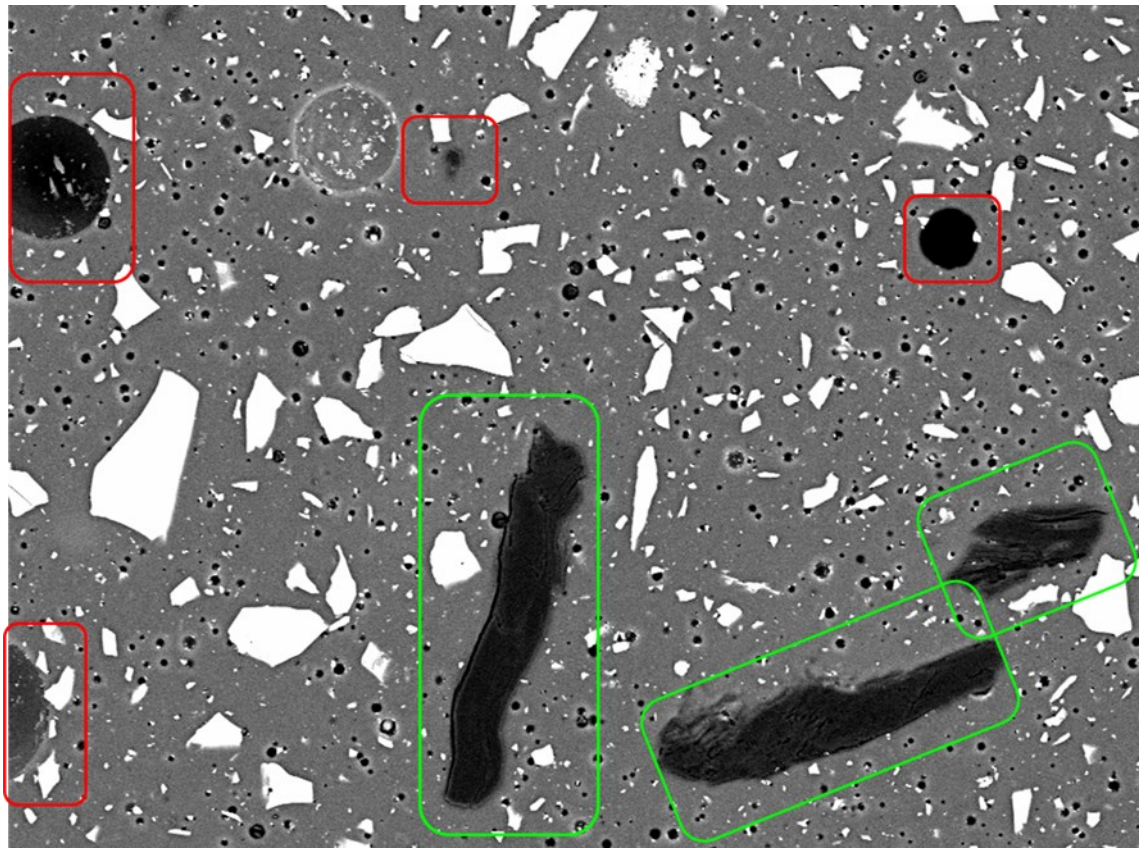

Figure 6: same level of grey between the graphite particles framed in green and bubbles in red

The objectives of the thesis is a continuation of the tests carried out previously. Indeed, the aim of this work is to develop a polished block preparation allowing the characterisation of graphite and, as changing the current recipe used at ULiège (addition of nanoparticles powder of black carbon as show in Figure 7) is not intended since it solves the problems associated with the traditional preparation without biasing the content of graphite in the following results (SEM), the work will focus on finding the cause of the exothermic reaction when the iodoform is added and improving the preparation either by minimising the reaction or suppressing it altogether.

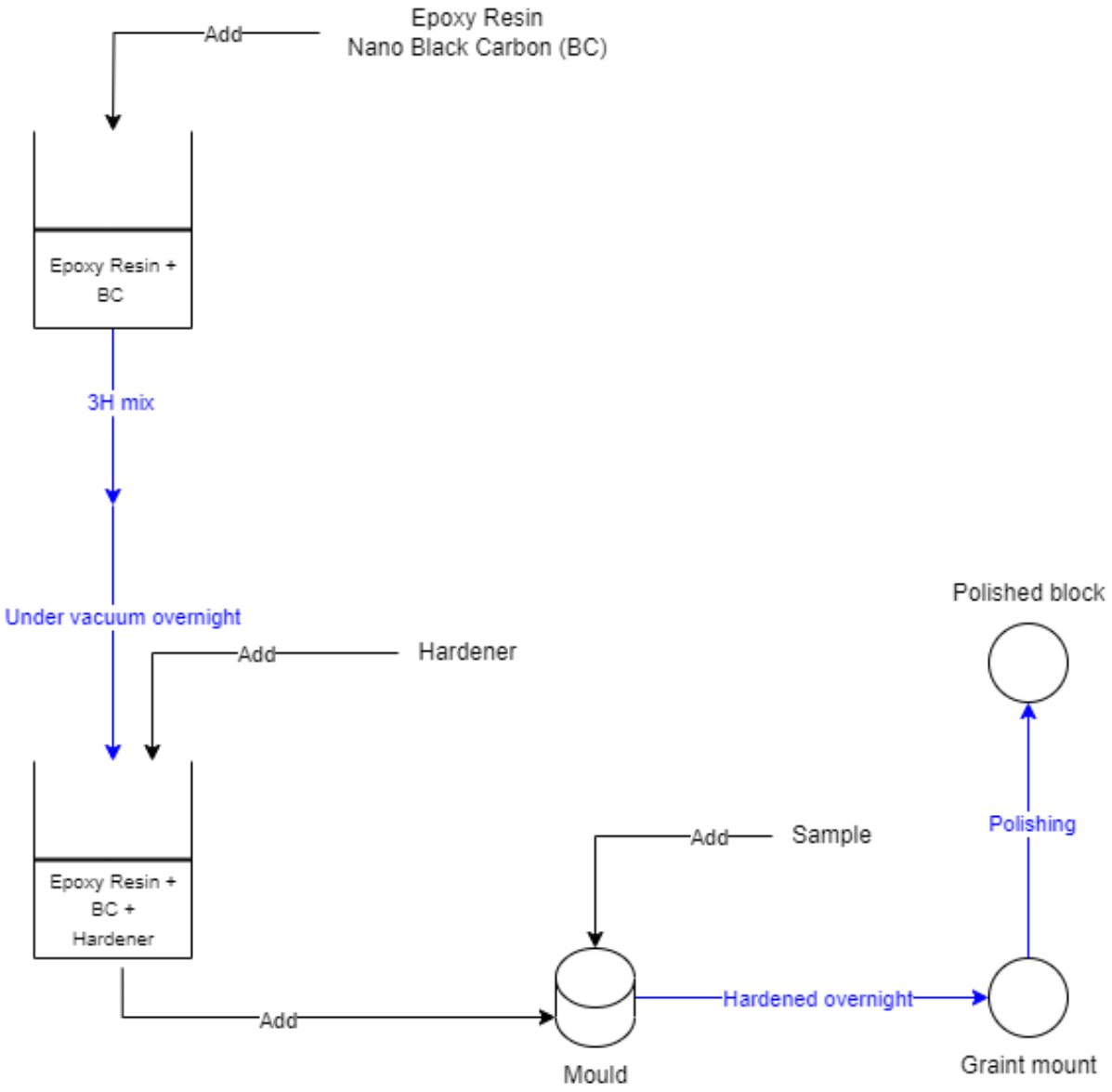

Figure 7: Schematic procedure for the preparation of polished block based on Bouzahzah et al. (2015) work

4 Material and methods

4.1 Material

The final samples which were analysed under the SEM after the refinement of the polished blocks preparation come from a gold mine containing native carbon which generates preg-robbing.

This mine contains gold encapsulated in sulphides, and therefore floats these sulphides to concentrate the gold. As a way to reduce the native carbon quantity and minimise pre-robbing, the mine floats the carbon just before the sulphide flotation.

The samples analysed in this project are therefore carbon concentrates from various carbon flotation trials using different combinations of frothers and the subsequent sulphur concentrates from the following sulphur flotation. This work was carried out with the aim of duplicating tests carried out in an external laboratory for verification of the results. The samples were first ground with a rod mill, then floated with the different combinations of frothers as indicated by the external laboratory procedures to concentrate the carbon first and then the sulphides. A total of 8 tests were carried out, resulting in 16 samples (one carbon concentrate and one sulphide concentrate per test). The products were then dried in an oven and finally divided. Part of the sample was sent to the analytical laboratory at the mine to obtain Au, Ag, total S, total C and As grades via chemical analysis. Another part was sent to ULiège for SEM analysis (sub-samples used for this project) although only 14 samples (7 tests) were finally received due to the low mass produced for the 8th test. The rest is stored at the mine.

The aim was to see which combination would allow to float the most carbon while losing the least amount of gold. However, the loss of gold is inevitable. It could be due to particles entrainment during the carbon flotation circuit, but it could also be related to the various associations with the other minerals in the crushed ore which can be seen by using microscopic observations (optical and SEM). Indeed, a small gold-bearing sulphide particles attached to a larger carbon source particle such as a graphite particle, may be floated, resulting in the loss of part of the gold.

4.2 Methods

4.2.1 Polished block preparation: development

4.2.1.1 Polishing method

The polishing process used in this project consists of 8 steps from a coarse abrasive disc to the final polishing step which is an abrasive particle size of 1 µm disc with a diamond suspension. The polishing machine used is Tegramin-30 from Struers (Figure 8). The list below shows the discs used (Struers) with details of abrasive particle size. The first five discs are used under water as a lubricant, and the last three are diamond-suspended.

- MD piano 120 (abrasive particle size of 125µm)
- MD piano 220 (abrasive particle size of 68µm)
- MD piano 500 (abrasive particle size of 30µm)
- MD piano 1200 (abrasive particle size of 15µm)

- MD piano 2000 (abrasive particle size of 7µm)
- MD-Largo (abrasive particle size of 9µm)
- MD-Dur (abrasive particle size of 3µm)
- MD-Dur (abrasive particle size of 1µm)

The last three steps are also the most time-consuming, taking from 7 to 15 minutes of polishing time, with immersing the polished blocks in an ultrasonic bath between each step to remove particles lodged in cavities, such as air bubbles and holes left by the removal of particles during the polishing steps (stripping of particles). The five first water-based polishing steps take no more than three minutes each.

Figure 8: Polisher Tegramin-30 from Struers

4.2.1.2 Preparation protocol of polished blocks on graphite bearing samples

The Figure 9 summarises all the tests carried out in this work, with a description given hereafter.

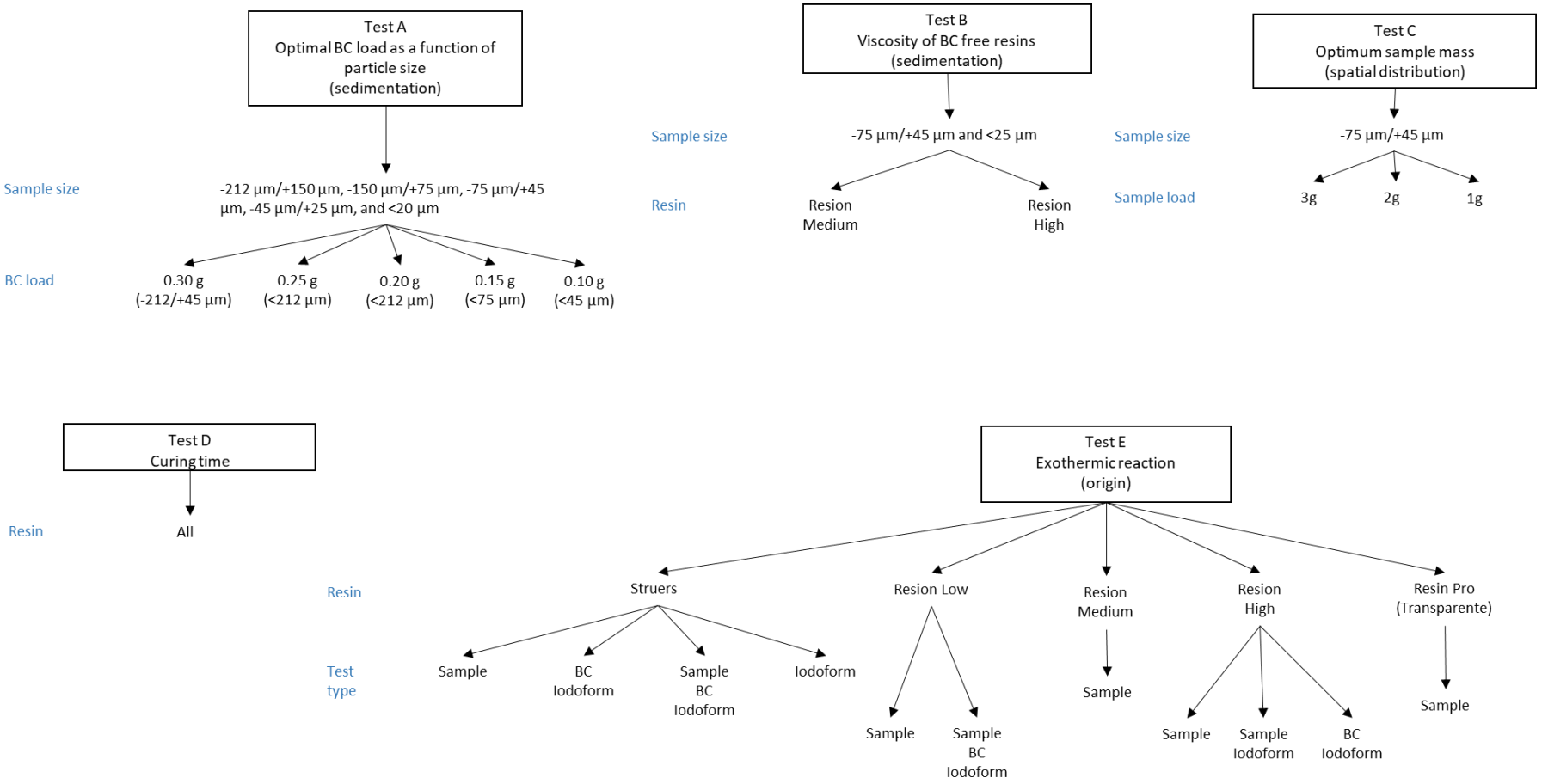

Figure 9: Summary of all tests conducted

1. BC load

As the aim of the work is finding the cause of the exothermic reaction, causing more air bubbles, when the iodoform is added and improving the preparation of polished blocks, a first idea was therefore initially to improve the current preparation (without iodoform) to minimize the creation of air bubbles. Indeed, the presence of air bubbles was already recurrent before adding iodoform to the preparation.

It is known that BC is agglomerated (see Figure 10) and contains a certain amount of air, therefore, after being mixed with the resin and put under vacuum to degas, some of the air released during the mixing may remain and contribute to the volume of bubbles present in the cured polished block. In other words, to reduce the air supply, it is necessary to determine the minimum charge of black carbon to be added to avoid sedimentation.

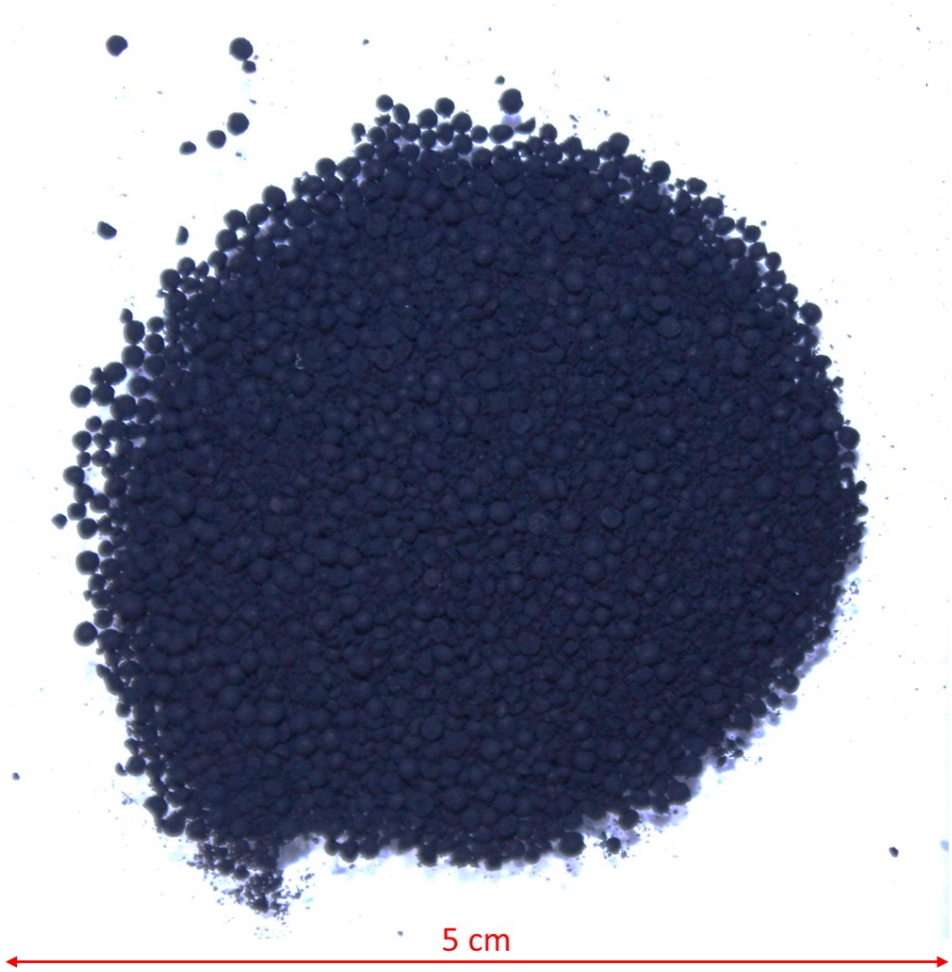

Figure 10: Image of nanoblack carbon particle aggregates (overexposed to light to illustrate the phenomenon).

The following tests were carried out using the usual ULiège procedure, i.e. without iodoform, with Struers EpoFix resin.

As sedimentation depends on particle density and size, a first test was carried out on a sample composed of quartz (80% by weight) and galena (20% by weight) with a particle size of less than 120 µm (galena: ~7.5 g/cm^3; silica: ~2.65 g/cm^3). The conclusion was that a load of 0.30 g of BC per polished block was sufficient to prevent sedimentation. This is why **test A**, which aimed to observe the sedimentation phenomenon as a function of particle size and BC load, began with a load of 0.30 g of BC. Initially, the test was based on a sample composed of particles ranging in size from -600 µm to +25

µm, and then samples with finer particle size ranges were used (-212 µm/+150 µm, -150 µm/+75 µm, -75 µm/+45 µm, -45 µm/+25 µm, and <20 µm).

In order to completely eliminate the air supplied by the BC, it was tested whether a resin more viscous than "Struers resin" could prevent particle segregation of the particles without the addition of BC. **Test B** was carried out on two samples: one with a particle size of -600/+25µm and one with a particle size of less than 25µm, to see whether BC was necessary to prevent sedimentation. The two more viscous resins chosen for each of these tests were "Resion Medium" and "Resion High" (Table 1).

2. Spatial dispersion

Another way of improving the initial preparation, which should have no influence on the possible exothermic reaction, is to determine the appropriate average charge of a sample for a polished block such that the analysis surface must not be too charged to prevent particles from coming into contact and biasing the release data. It should also contain enough particles to ensure that the sample is representative when measured. **Test C** was realised on a sample with a granulometric range of -75 µm/+45 µm only.

3. Using different resins brands

What is causing the exothermic reaction: is it the resin-BC-iodoform mixture, the BC-iodoform mixture, or the resin-iodoform mixture? As the exothermic reaction was obtained with Struers EpoFix resin, it was decided to test other brands of resins available on the market and compare them with Struers resin. Curing time, predisposition to exothermic reaction (with and without sample), and possible exothermic reaction between the resins and other materials (iodoform and BC) were analysed. Table 1 shows the resins brands used with the corresponding ratio for the resin-hardener mixture given in mass.

Table 1 : List of resins with corresponding ratio.

Name	**Ratio resin-hardener (by mass)**
Eco Epoxy Resin (Clear) from Epodex	2:1
Pro Epoxy Resin (Ultra Clear) from Epodex	2:1
Transparente Epoxy Resin from Resin Pro	100:60
UV Resin Art Epoxy EP 102 (Low viscosity) from RESION	2:1
UV Resin Art Epoxy EP 103 (Medium viscosity) from RESION	2:1
UV Resin Art Epoxy EP 104 (High viscosity) from RESION	2:1
EpoFix Resin from Struers	100:12
ICRYSTAL 5-FIVE Epoxy Resin from Resin Pro	100:67

Test D consisted in determining the curing time of the resins under atmospheric pressure and in a vacuum, in order to be able to discriminate between those that would take too long. The tests consisted of mixing the resins with the corresponding hardener (in the ratio specified by the vendor). In addition, it was also possible to see whether or not the resin was predisposed to an exothermic reaction under the effect of vacuum or atmospheric pressure. Each resin was cured in a 30mm diameter mould.

Test E first investigated the origin of the exothermic reaction for “Struers resin”: it was determined by making a mixture containing resin, material (sample), BC and iodoform, a material-resin mixture, a resin-iodoform mixture alone and a resin-BC-iodoform mixture. These were made in ambient air (atmospheric pressure) and under pressure (non-atmospheric, around 2.5 bar) to see if there was any difference. The mixture of the other resins that had cured overnight and a material to see if this mixture could trigger an exothermic reaction was also investigated. The two extreme viscosity resins from Resion (“Resion Low” and “Resion High”) were further tested to compare with the results of “Struers resin”.

4.2.2 Automated Mineralogy analysis – how does it work?

Scanning Electron Microscopes are used in various fields such as biological and material sciences, art, mining, etc. The principle consists of an electron beam propelled at high-speed point by point over a sample, all carried out in a high vacuum. The purpose of the vacuum is to minimise the scattering of the electron beam before it reaches the sample. The interaction of the sample with the incident electron beam generates a variety of secondary signals. The generated secondary signals are Backscattered Electrons (BSE), Secondary Electrons (SE), Characteristic X-Ray, Diffracted Backscattered Electrons (EBSD), and Cathodoluminescence (CL). They allow samples to be imaged with a resolution of up to 1nm, providing information on topography, morphology, crystallography, and chemical composition when combined with an Energy Dispersive Spectrometer (EDS). The Figure 11 illustrates the general schematic form of a SEM.

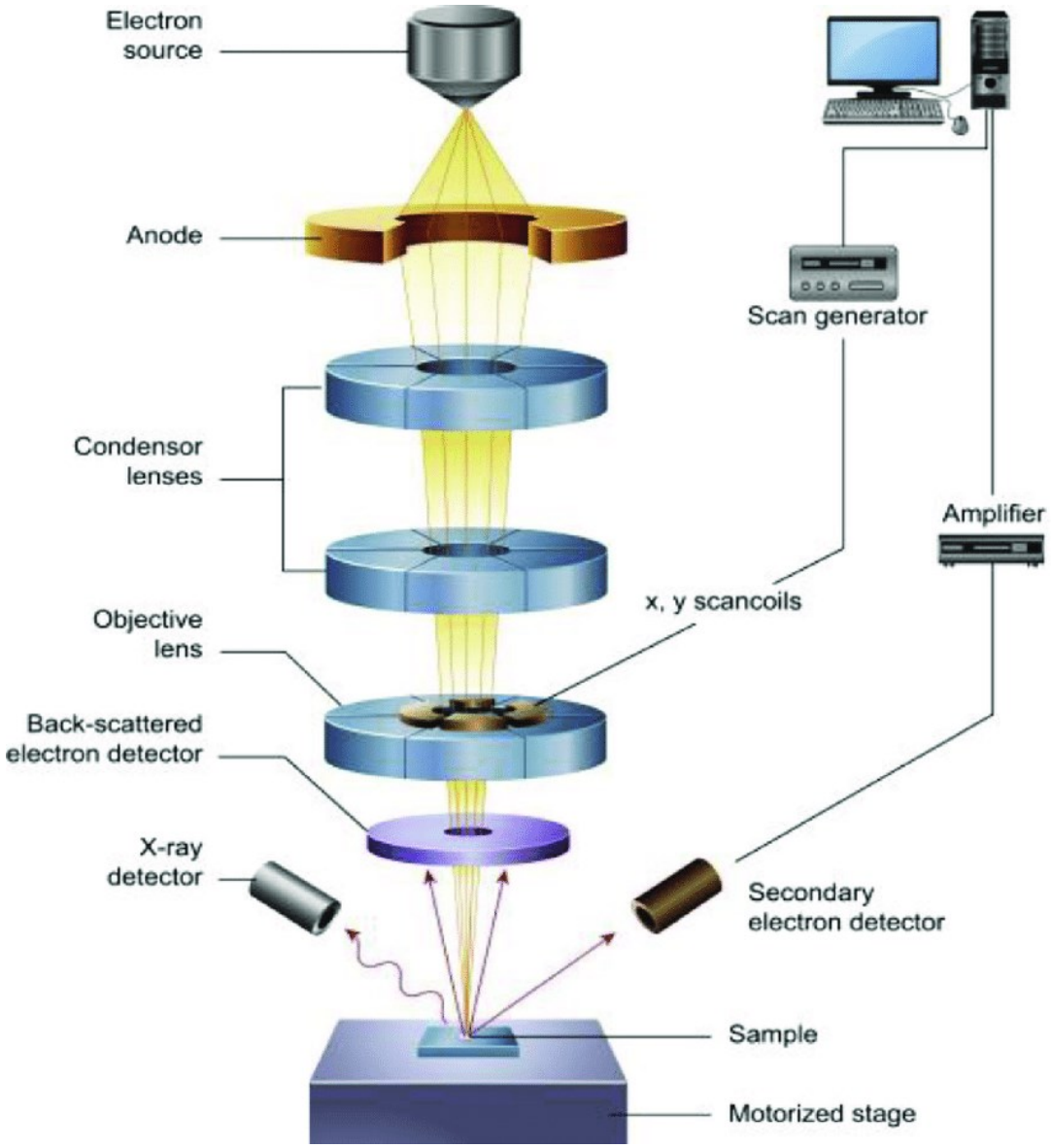

Figure 11: Schematic form of SEM (from Ali, 2020)

The interactions between the material and the electron beam that produce the secondary signals take place within a certain interaction volume, which is pear-shaped (Figure 12). The interaction volume depends on the atomic number (Z) of the sample and the acceleration voltage (kV) of the electron beam: as the acceleration voltage increases, the penetration depth increases; as the atomic number increases, the interaction volume decreases.

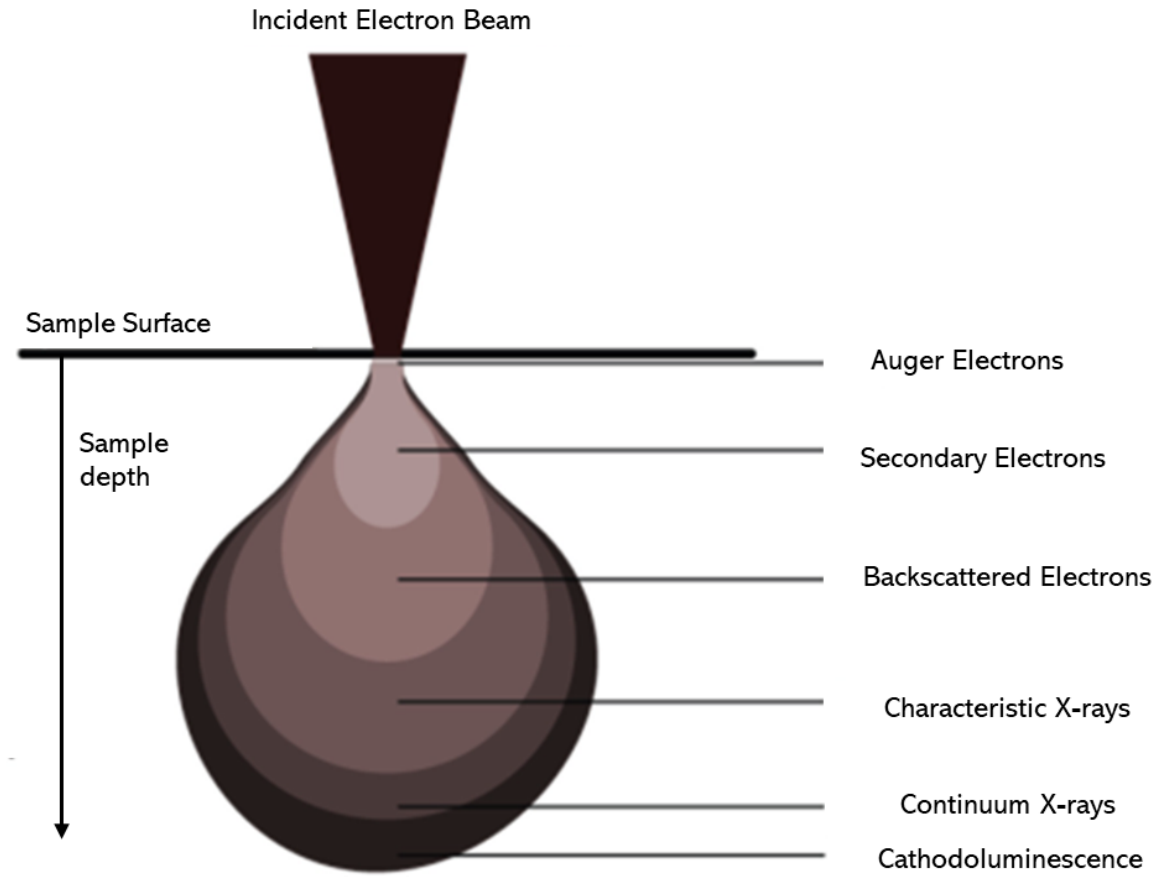

Figure 12: Interaction volume (modified from Ul-Hamid, 2018)

Below is a description of some of the signals that can be analysed by SEM:

- Secondary electrons (SE):

They provide surface details and topography. These electrons are re-emitted from the sample by the phenomenon of inelastic diffusion and therefore have a lower energy (<50eV). This is also why they come from the surface of the sample (a few nm deep). As the detector is placed on one side of the sample, the electrons emitted on the opposite side are not detected, which has the effect of accentuating the relief by creating a shadow zone.

- Back scattered electrons (BSE):

They give chemical contrast (greyscale) allowing imaging. These electrons are re-emitted from the sample by elastic diffusion and therefore have a higher energy than SE electrons (>50eV). They thus come from a greater depth (>100nm). The higher the atomic number (or average atomic number), the greater the number of BSE emitted, making the sample appear brighter. The detector is placed just above the sample, as BSE is mainly emitted upwards.

- X-Rays:

They offer chemical data. When the sample is bombarded by the beam, the energy of the incident electrons may be sufficient to eject electrons belonging to an inner electron layer of an atom in the sample, leaving a gap in the layer. The atoms in the sample therefore go into the excited state, causing an electron in an outer layer to "jump" to fill the vacancy by releasing excess energy. A characteristic X-ray equivalent to the energy change in the "jump" is generated. As each chemical element has an X-ray

fingerprint, the X-rays detected by an Energy Dispersive Spectrometer allow qualitative analysis (energy of the peak) and quantitative analysis (intensity of the peak). The characteristic X-rays can come from a greater depth than the BSE (up to about 3 µm).

The use of the SEM can also be automated as an Automated Material Characterisation system, which is then called a SEM-based Automated Mineralogy (SEM-AM). SEM-AM results then from the combination of a hardware platform (=SEM) and a specific image analysis and processing software (mainly using backscattered electron imagery and energy dispersive analysis) and as mentioned above, this enables a significant number of mineral grains to be analysed in order to represent the sample as accurately as possible and to generate particle-specific data for subsequent interpretation.

Several Automated Mineralogy systems have been developed, including : MLA (Mineral Liberation Analyser) whose classification is based on the characteristic X-ray spectra of mineral species which are compared with a library of reference spectra; QEMSCAN (Quantitative Evaluation Minerals by Scanning Electron Microscopy) whose classification is the same as for LMA; TIMA (TESCAN Integrated Mineral Analyser) whose classification is almost the same as for LMA (high counts instead of low counts due to the summation of low-count spectra for each pixel in segments with the same BSE); Mineralogic Mining system (ZEISS) whose classification is based on quantitative measurement of the chemical composition of minerals, i.e. it automatically detects the elements present in any X-ray spectrum for each pixel analysed and then calculates the quantitative abundance of each element which allows for mineral; …

4.2.2.1 Equipment used

In this project, samples mounted in a polished block can be first imaged using an optical microscope (Zeiss AxioImager M2m) with an XYZ motorized stage to obtain a complete tiled images that allows the sample to be navigated under the Scanning Electron Microscope with micrometric precision thanks to correlative microscopy.

Before having their entire surface imaged by the SEM, the polished blocks are first coated with a thin layer of carbon to ensure conductivity which allows the evacuation of the flow of electrons accumulating in the sample. Particle phases are analysed by the SEM using a Zeiss Sigma (300 field emission gun) equipped with two Bruker (xFlash 6|30 X-ray) Energy Dispersive Spectrometers (as seen in Figure 13). SEM-EDS analyses were performed under vacuum using a probe current of 2.3 nA with an accelerating voltage of 20 kV at a working distance of 8.5 mm. This working distance is kept fixed to ensure that the surface always has the same grey level of the BSE image with the saved defined parameters such as brightness, contrast, and calibration. During this work, copper was used as a reference material for calibration.

Under fixed parameter, a BSE image can be collected in which the resin can be distinguished from the particles before mapping each particle thanks to the ZEISS Mineralogic Mining automated mineralogy software that enables the use of a backscattered electron thresholding. This software also offers different analysis modes: mapping analysis, spot centroid analysis, feature scan, line scan, and BSE only.

To enable a complete analysis of the sample, mapping analysis will be used. The time required for measurement is controlled by user-defined parameters such as step size (pixel size), EDS dwell time (which adjusts the counts per EDS pixel), number of analysis points and/or number of particles (sample surface) to be measured. The EDS step size and magnification for the analysis allow the software to draw the analysis grid. Other tools can be used to process the image, such as the use of size limits (minimum or maximum), the ability to remove particles touching the edges of the frame or to stich

particles cut between several frames, etc. Measurements related to particle size and shape (e.g., area, elongation, ferret maximum diameter etc.) are visual information which are extracted by the software from the BSE images stored during the images collection.

Afterwards, the classic point-counting method is applied by the system. The identification of the mineral or phase is then determined using a classification file developed from a prior optical study and the collection of X-ray spectra from the first analysis.

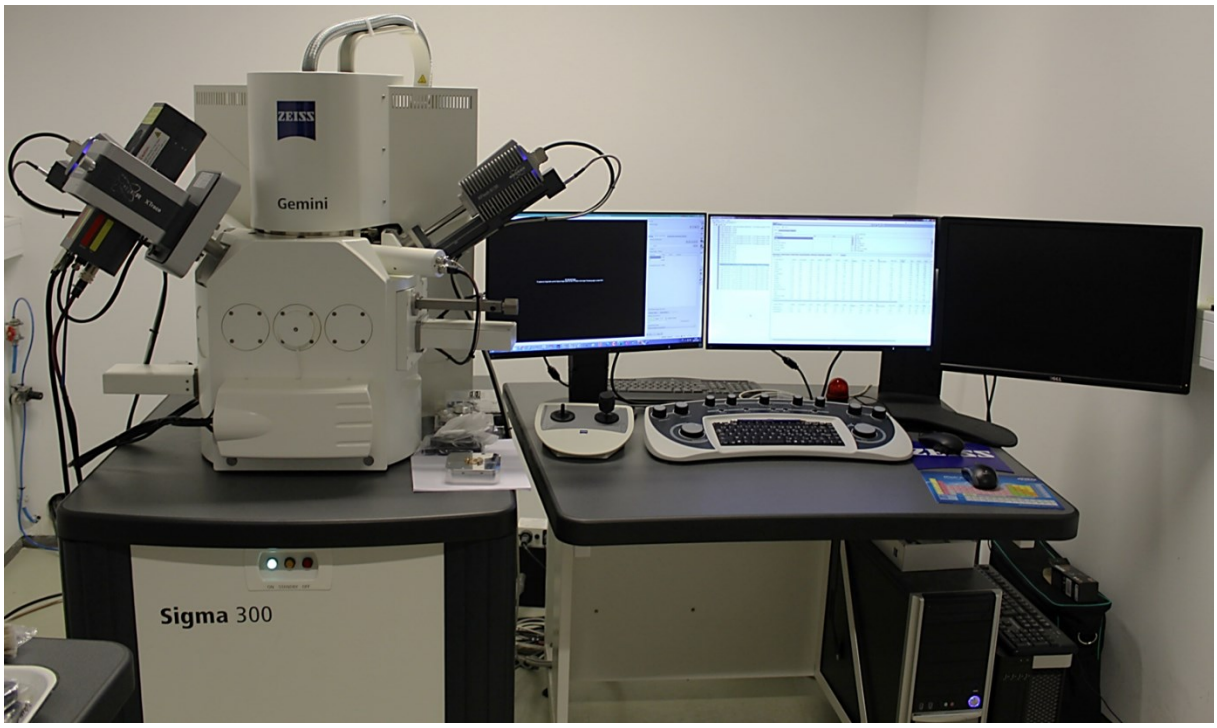

Figure 13: SEM-based Automated Mineralogy (Equipment used)

4.2.2.2 Automated mineralogy programming

4.2.2.2.1 Threshold method

The Mineralogic allows to consider only the minerals, by eliminating the resin which is darker (in grey levels), with a method allowing to apply a threshold. Only elements between two chosen thresholds are considered. The thresholds are given in greyscale (0-255). Using iodoform, there should be a good contrast between the graphite, the resin and the rest of the minerals. With the double threshold function of the Mineralogic, graphite that is darker than the resin and other minerals that are lighter can be distinguished from the resin. As a result, the resin will not be analysed.

To do this, the SEM is placed over a frame containing sufficient graphite and other minerals, such as silicates. On the Mineralogic, it can then be viewed from the double threshold function three peaks. One represents graphite (the leftmost, peak number 1 in the Figure 14), another, which is often higher, corresponds to the resin (in the middle, peak number 2 in the Figure 14) and the last one represents the other minerals (the rightmost, peak number 3 in the Figure 14). On the first double threshold, it is therefore necessary to include the peak representing graphite, and on the second to include everything else after the second peak representing resin, so as to avoid selecting it. The selection is easily visible on the image thanks to the colouring of the elements selected by the double thresholding. For example,

in the Figure 14, it can be seen that minerals with a grey level between 118 and 255 on the grey scale are selected in green.

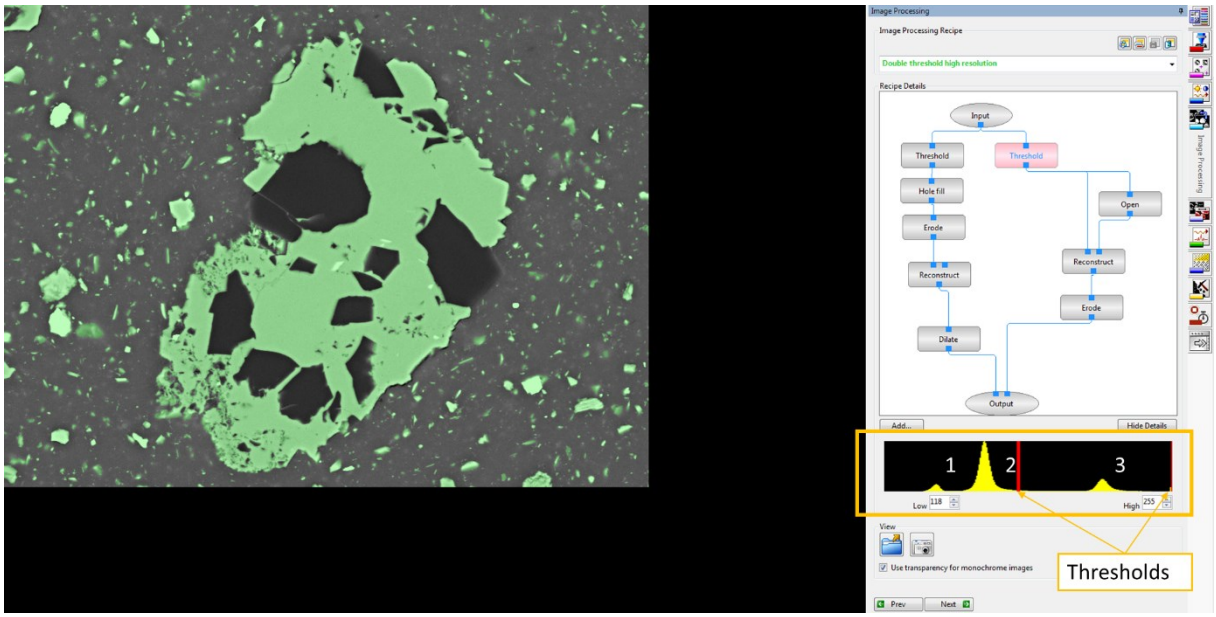

Figure 14: Thresholding method, example with a selection between 118 and 255 on the grey scale. Display of the 3 peaks, with 1 corresponding to graphite particles, 2 corresponding to the resin and 3 corresponding to the other minerals

Figure 15 below shows the result of double thresholding. Graphite and the other minerals are selected (and can therefore be analysed by the Mineralogic) while the resin is not selected.

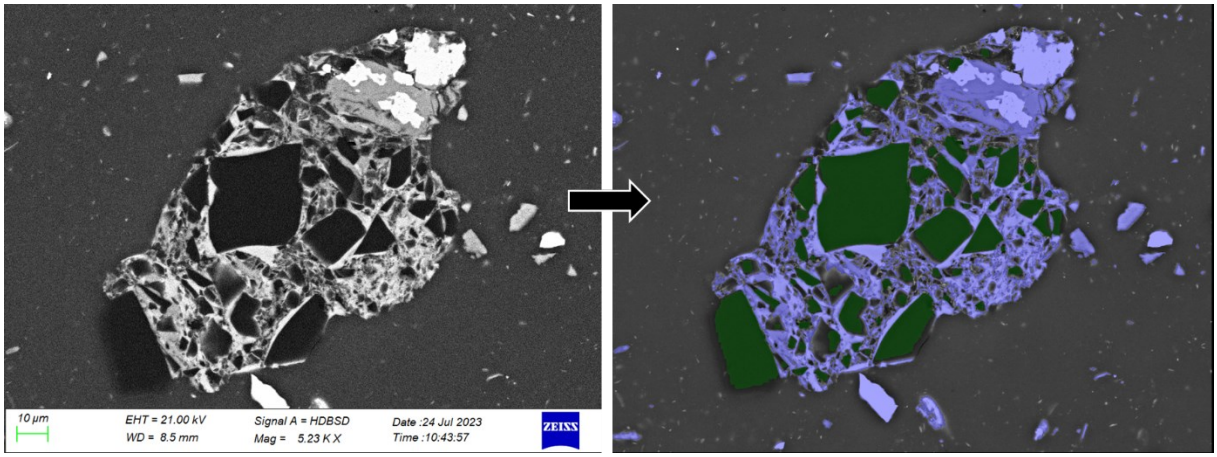

Figure 15: Result of a double thresholding. Graphite particles selected in dark green, other minerals in blue

If the surface is not polished properly, a relief may be created in certain places. This is because the resin, which is softer, deepens at the edge of a more resistant grain during polishing. However, this relief has the same grey level as graphite and appears as an "edge" around some minerals as shown in the Figure 16. This biases the liberation results. It is thus necessary to refine the image processing. To do so, a limit was placed on the size of the grains analysed by the automated system, such that grains whose size is less than 7 µm are not taken into account (for all minerals).

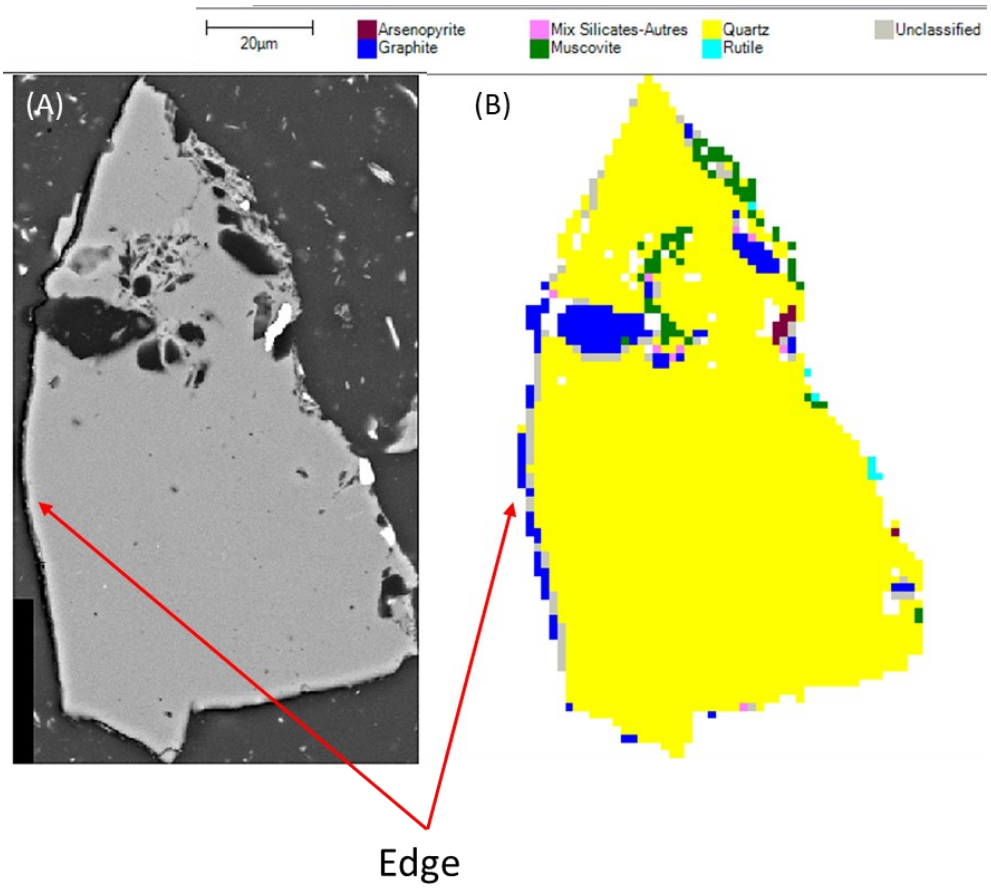

Figure 16: On the left (A), edge in black (same grey level as graphite); on the right (B), edge analysed as graphite in blue

4.2.2.2.2 Creation of the mineralogical database

Mineral classifications are generally carried out using a combination of the BSE image and the EDS spectra, which have been deconvolved to give the weight % contribution of the elements (quantification). It is therefore possible to set minimum and maximum percentages around the ideal stoichiometric composition of the mineral for each element forming it. Elemental ratios can also be applied to distinguish phases which have a solid solution. Each mineral classification requires the addition of specific gravity, which is used in a series of calculations, e.g. modal mineralogy (Graham *et al.*, 2015). It is also possible to add a minimum and maximum grey level value derived from the BSE image of the mineral.

Figure 17 below shows an example, quartz. It can be seen that oxygen (O) and silicon (Si) have been selected. The minimum values for stoichiometry have here been set at 20% for both. This means that any pixel whose deconvolved spectrum shows at least 20% O and Si is placed in the "quartz" category. Quartz is therefore generally placed at the end of the list of minerals because the software compares the data with each classification and the first one whose data satisfies corresponds to the class of the pixel. Minerals with more restrictions, such as more elements needed to validate them, are placed at the top of the list. The specific gravity and grey level have also been indicated. Finally, a colour is assigned to distinguish the minerals when the particles are "mapped".

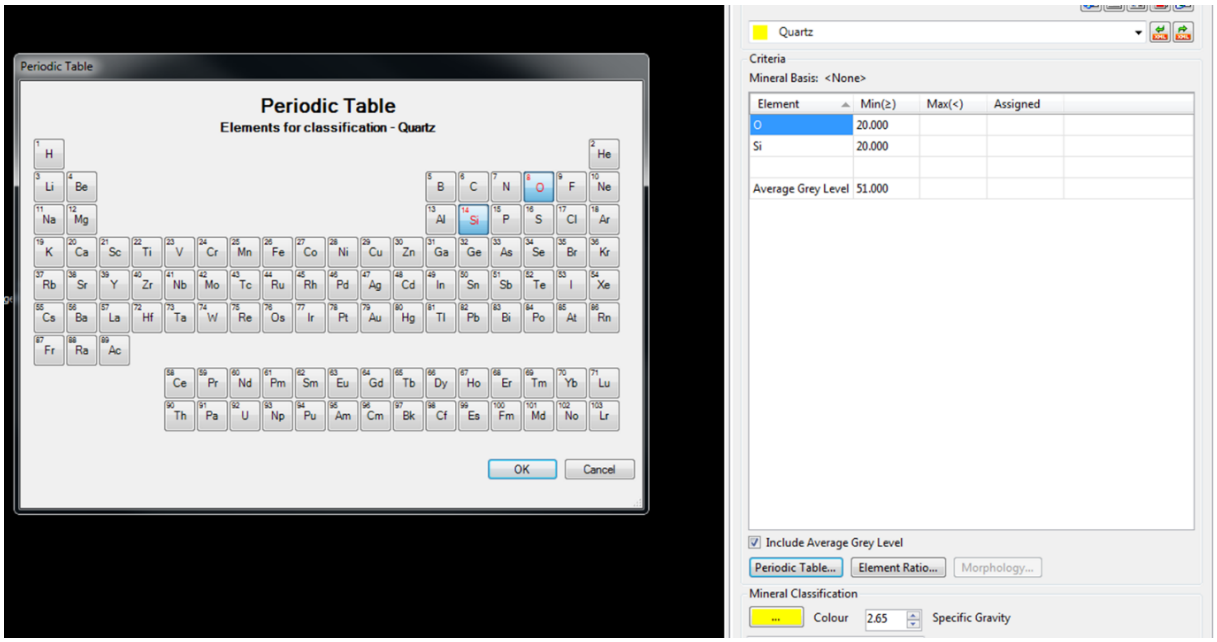

Figure 17: Mineralogic classification window

During this project, three types of classification files were considered:

- The first classification deconvolved element C (carbon) from the spectrum, even though usually C is not, because if it were, it would "dilute" the wt% of the other elements due to the resin being rich in carbon and thus the stoichiometry of the mineral is further from the ideal one. This could make it difficult to differentiate between minerals with similar "diluted" stoichiometry.
- Another classification did not deconvolve C, which meant that the stoichiometry of the minerals was closer to the ideal one. To classify graphite, a limit on the grey level has been added so that each pixel with a level smaller than it, is classified as graphite.
- A final classification was to deconvolve the C and add a limit on the grey level for each mineral, i.e., graphite was below a said level and other minerals were above this level.

5 Results and discussion

5.1 Results of the chemical analysis of the samples

Table 2 below shows the different samples references, their chemical composition (obtained from the mine laboratory) and whether they are carbon concentrate (CC) or sulphide concentrate (CS). Each CS is placed on the following line of its corresponding CC.

Table 2: Chemical analysis of samples (grades)

Frothers combination - test reference	Sample reference	Type of concentrate	g/t Ag	g/t Au	%S TOT	%C TOT	%As
1	G1077	CC	5.1	4.7	4.0	14.6	0.8
	G1090	CS	15.5	36.5	23.5	3.1	5.8
2	G1078	CC	5.5	3.8	3.2	11.8	0.7
	G1091	CS	11.9	32.9	21.1	3.2	5.4
3	G1079	CC	7.4	4.4	3.6	12.4	0.7
	G1092	CS	11.3	31.2	20.6	3.3	5.3
4	G1080	CC	10.3	5.6	3.7	11.1	0.9
	G1093	CS	10.1	32.0	26.1	2.4	6.3
5	G1081	CC	4.9	5.8	4.6	12.7	1.1
	G1094	CS	13.7	28.5	20.5	2.7	6.1
6	G1088	CC	3.7	3.6	3.4	10.3	0.7
	G1095	CS	13.6	34.0	21.9	2.7	5.4
7	G1089	CC	4.1	2.7	2.5	9.2	0.5
	G1096	CS	11.1	29.0	20.9	3.3	5.4

Given that the aim of this project is to develop a method for characterising graphite using an automated mineralogy system, discussion of how the flotation tests were carried out (are they good duplicates?), and which combination of frothers is best for achieving the flotation objectives will not be discussed here. Thus, only the results of the chemical analyses are given in order to be able to discuss the new method developed in this project.

5.2 Results of the polished block preparation

A total of about 80 polished blocks were produced for the following tests. Those are discussed hereafter.

Reminder of the tests (Table 3):

Table 3: Tests reference with short description

Test reference	Short description
Test A	Optimal BC load as a function of particle size
Test B	More viscous resins on a sample with a wide particle size range and on a sample with a particle size range <25 µm, without BC
Test C	Optimal sample mass for a better spatial dispersion
Test D	Curing time of different resins (resin-hardener only)
Test E	Study of the origin of the exothermic reaction

5.2.1 Determination of the minimum BC load to avoid sedimentation

Most of the polished blocks prepared for the following tests required to be cut on the height and remoulded to make a vertical section in order to observe the possible sedimentation. For each test, the vertical section was analysed under the optical microscope to determine whether or not the particles sedimentation has occurred.

Additionally, a pressure of about 2.5 bar was applied on the polished blocks via a pressure vessel during curing. Indeed, during previous tests carried out at the ULiège, it had been demonstrated that this additional step allowed to eliminate or strongly decrease the size of the bubbles in the block (Figure 18).

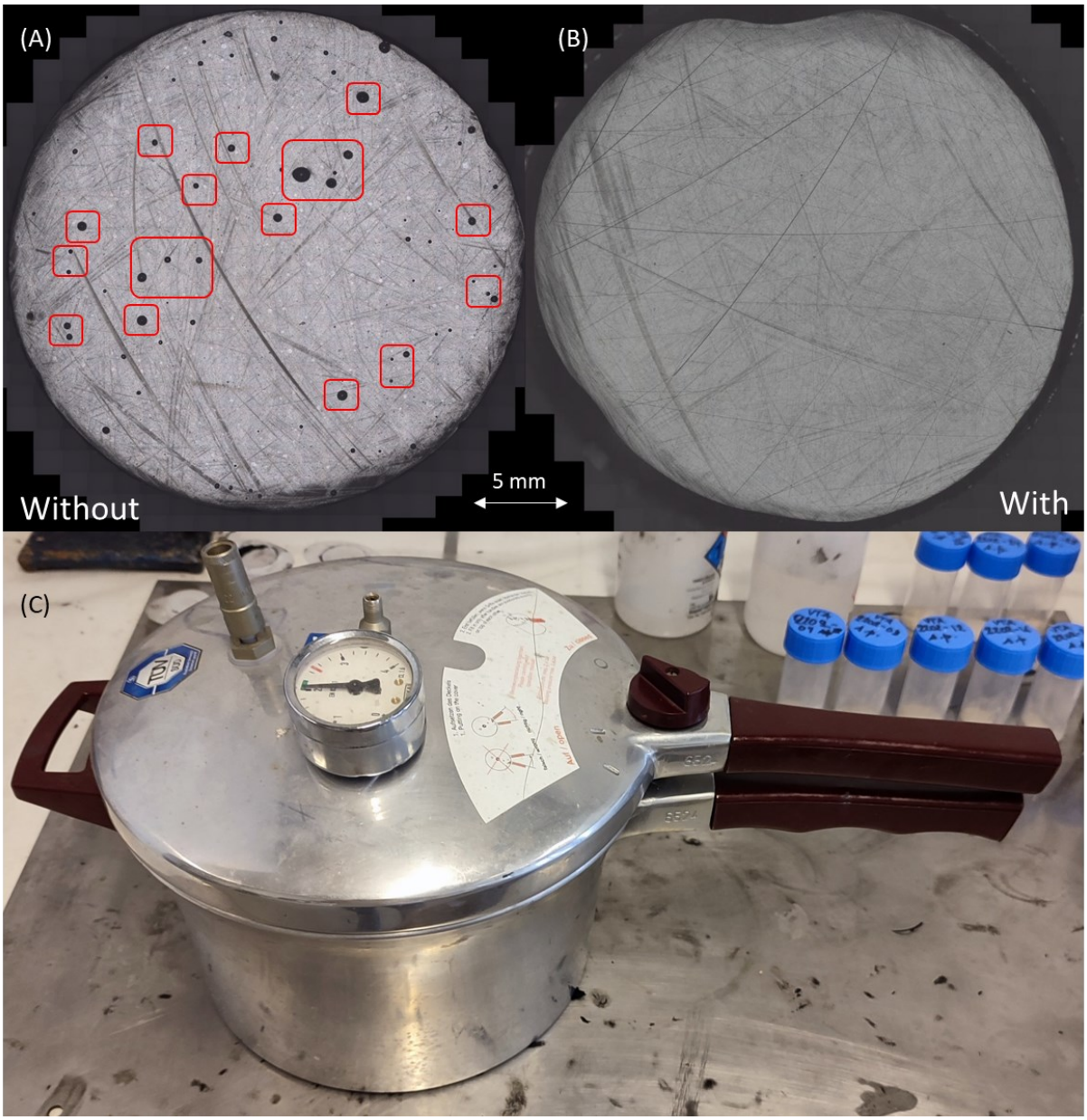

Figure 18: Top right (A), polished block cured without pressure vessel where air bubbles are occurring; Top left (B), polished block cured under pressure vessel which removed all air bubbles; Bottom (C), pressure vessel

i. Test A

The purpose was to observe the sedimentation phenomenon as a function of particle size (sample with a particle size range from -600 µm to +25 µm) and BC load. The BC loads were 0.30g, 0.25g and 0.20g. The tests started at 0.30g, based on the conclusion of a previous test. As can be seen from the Figure 19, the larger particles tend to be more concentrated in the lower part of the block (beginning of settlement) whereas for the finer particles no particular behaviour is apparent, i.e., there seems to be no settlement at all. For this reason, it was then decided to work by finer particle size range to determine the optimum BC load for each range (-212 µm/+150 µm, -150 µm/+75 µm, -75 µm/+45 µm, -45 µm/+25 µm, and <20 µm).

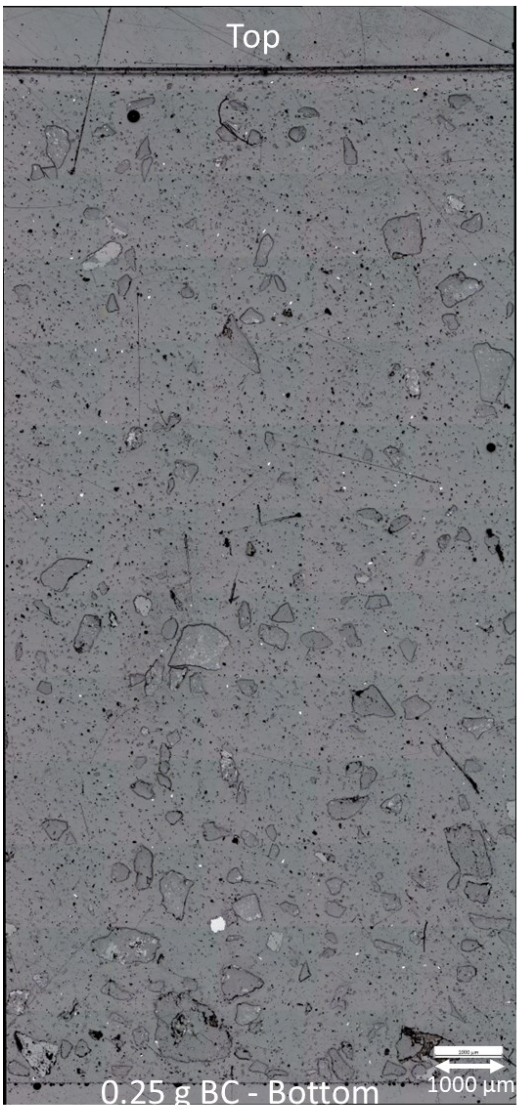

Figure 19 : Vertical section with sample mix (+600/-25 µm) and 0.25 g of BC

Each particle size range was tested with different BC loads, and the polished blocks were analysed under the optical microscope test to determine the optimum load to avoid grain sedimentation.

Below are the results for the -212/+150 µm particle size range, analysed using SEM and the Mineralogic software to produce a more illustrative figure (Figure 20). It can clearly be seen that for a load of 0.25 g of BC (L50) there is the beginning of settling.

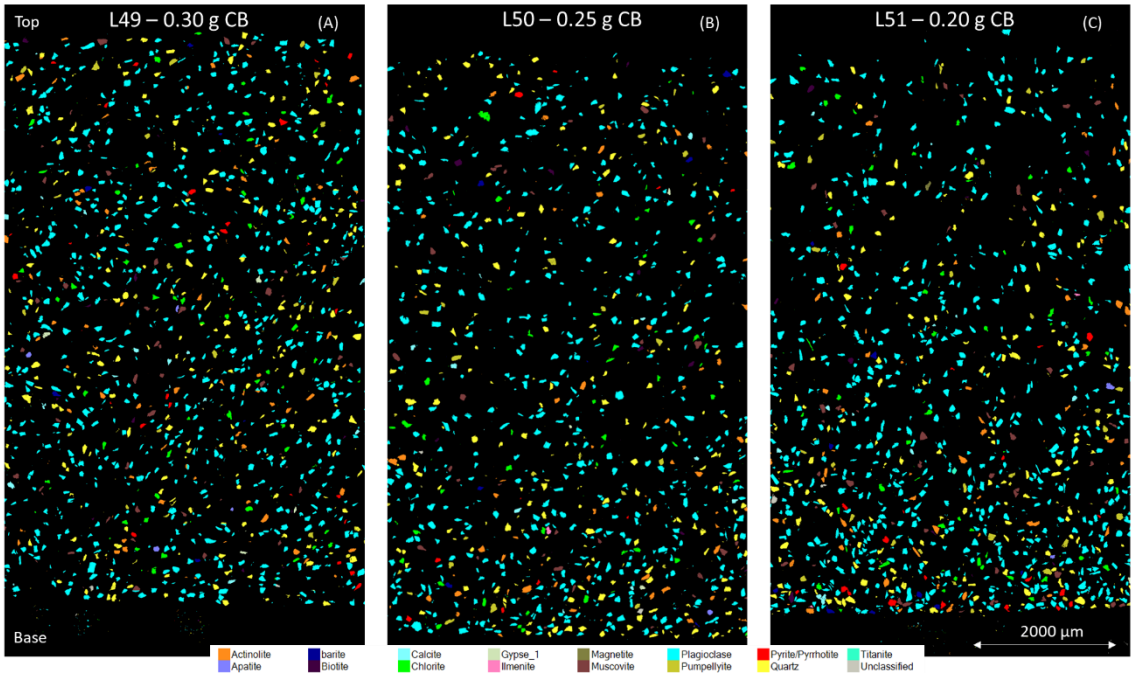

Figure 20: Analysis using the SEM and Mineralogic software of the -212/+150 µm fraction. No sedimentation for 0.30 g of BC (A). Beginning of sedimentation for a load of 0.25 g of BC at the base of the polished block (B). Visible sedimentation for 0.20 g of BC (C)

With the results of these tests, a summary table (Table 4) on the optimal BC mass to add can be created according to the particle size of the sample to be mounted in polished block.

Table 4 : Optimal BC load according to particles size range of sample

>75 µm	75-45 µm	45-25 µm	<20 µm
0.30 g BC	0.25 g BC	0.20 g BC	0.10 g BC

ii. <u>Test B</u>

As it was thought that a more viscous resin might help avoid the segregation of particles without adding BC, the Medium and High viscosity resins from RESION were chosen for those both series of tests.

The first series of polished blocks were made using a sample with a particle size ranging between -600µm and +25µm and, a sample with a particle size under 25µm, to see if BC was necessary to prevent sedimentation.

For the resin blocks with the large particle size range, it is evident that there was sedimentation at the base of the block during the curing time (see Figure 21).

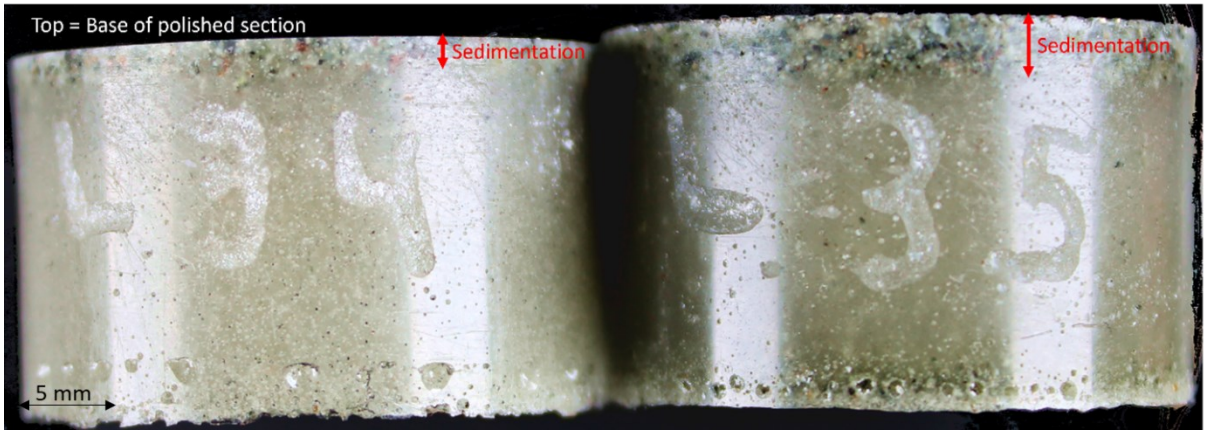

Figure 21: Polished blocks with sample mix (+600/-25 µm) without BC

However, for the polished blocks with a sample whose size is less than 25 µm, the two resins used alone (without BC) were sufficient to avoid settlement. This result was to be expected as with the "Struers resin" which is less viscous than those used in those resin blocks, particles smaller than 20 µm required only about 0.10 g of BC per block to have a good dispersion of the sample over its entire height.

In other words, with a more viscous resin such as Resion (High or Medium viscosity), it is not necessary to add BC for a particle size inferior to 25µm. This also avoids introducing air into the block due to the three hours BC mixing.

5.2.2 Determining the mass of the sample for a better spatial dispersion

iii. Test C

This test used a sample with a granulometric range of -75 µm/+45 µm only. The results obviously depend on the type of sample used: composition, density, particle size range, etc. For the one used, it turned out that for a particle size range of -75 µm/+45 µm, one to two grams of sample was the optimum, as shown in the Figure 22. In fact, 3 g of sample (L69) seems too loaded for a good analysis, while 1 g and 2 g of sample (L70 and L71) have particles that are more widely spaced, so a load of between 1 and 2 g seems to be a good compromise.

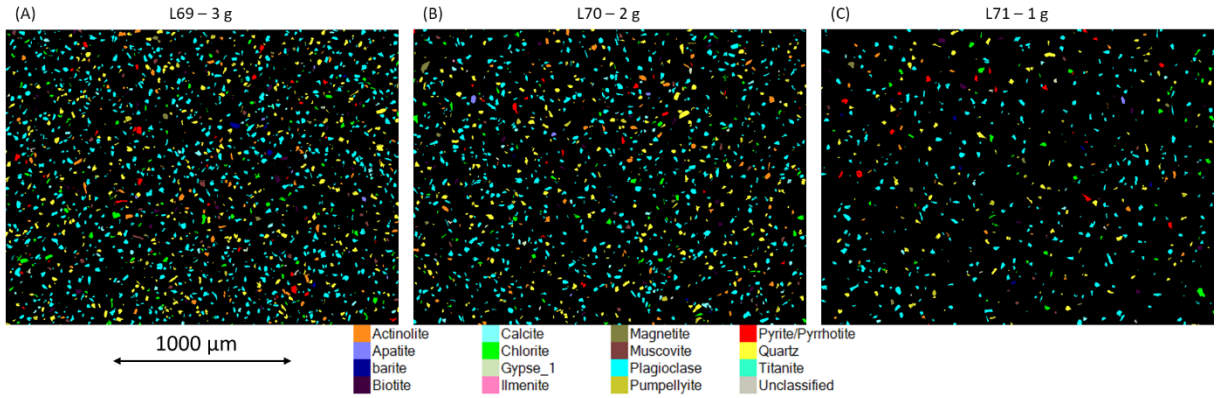

Figure 22: (A) Spatial dispersion for 3g of sample; (B) Spatial dispersion for 2g of sample; (C) Spatial dispersion for 1g of sample

5.2.3 Origin of the exothermic reaction

Figure 23 : Resins

iv. Test D

Firstly, it was necessary to compare the curing time of the resins (see Figure 23), under atmospheric pressure and under vacuum. Of all the resins tested, only the RESION resins (Low, Medium and High viscosity), the Transparente resin from Resin Pro and the “Struers” resin hardened after one night. The Icrystal 5-five resin hardened after two nights and, the Clear and Ultra Clear resins from Epodex after three nights. Below (Figure 24), it can be seen the cured appearance of the different resins which were ready after one night.

The Figure 24 shows that the resins cured under vacuum have fewer air bubbles. There does not appear to be any exothermic reaction when the mould is placed under vacuum. However, under atmospheric pressure, the resins show much more air bubbles. The air bubbles present are drawn into the resin when the hardener is mixed with it. The fact that there are more bubbles when the resin block is left to cure in ambient air can be explained by the fact that the vacuum extracts a certain volume of bubbles before complete curing. In ascending order of the volume of bubbles, there are “Resion Low”, “Resion Medium”, and finally “Resion High”. A more viscous resin shows more bubbles, which means it “traps” the bubbles. It has also been found that, of the Resion resins, “Resion High” cures faster than “Resion Medium” and “Resion Medium” cures faster than “Resion Low”.

The Figure 25 illustrates the cured appearance of “Resin Pro Transparent” resin under vacuum and atmospheric pressure, as well as “Struers” resin under vacuum only, for comparison. Here again, when the mould is left in the ambient air, there is more air bubbles.

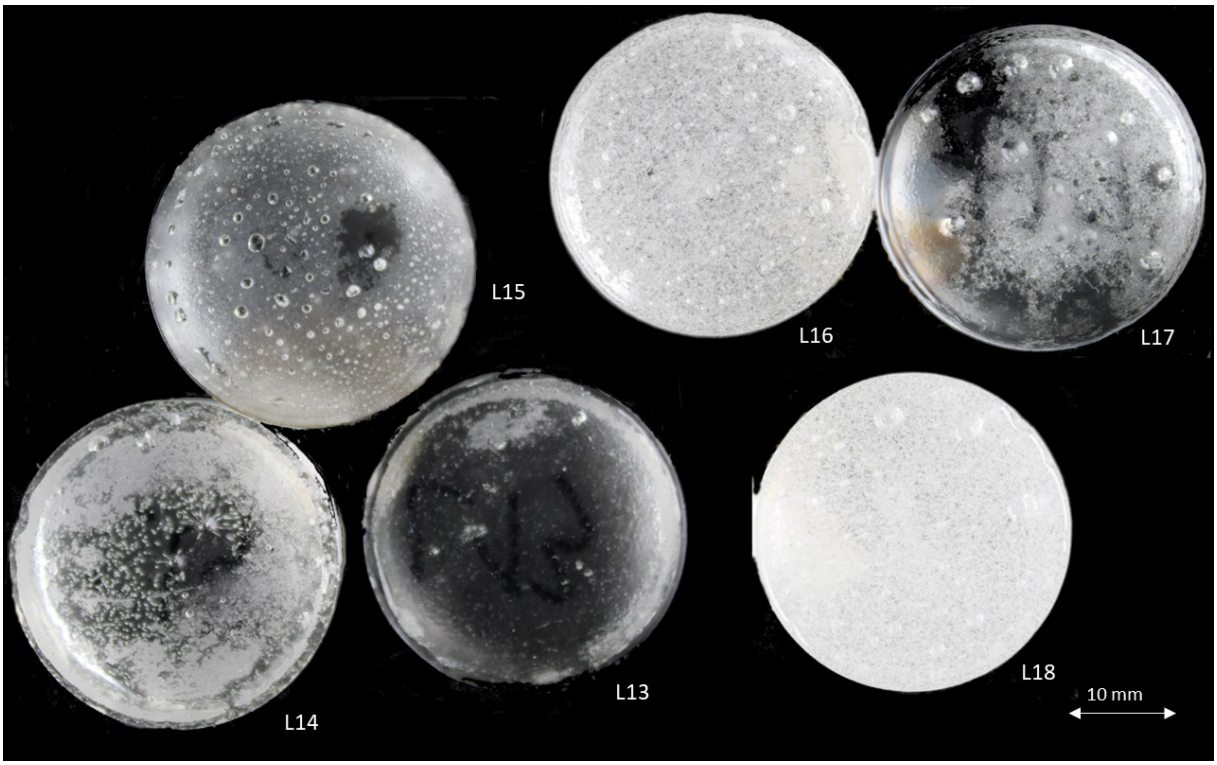

Figure 24 : L13 = Resion Low (vacuum), L14 = Resion Low (atmospheric pressure), L15 = Resion Medium (vacuum), L16 = Resion Medium (atmospheric pressure), L17 = Resion High (vacuum), L18 = Resion High (atmospheric pressure) – 30 mm diameter mould

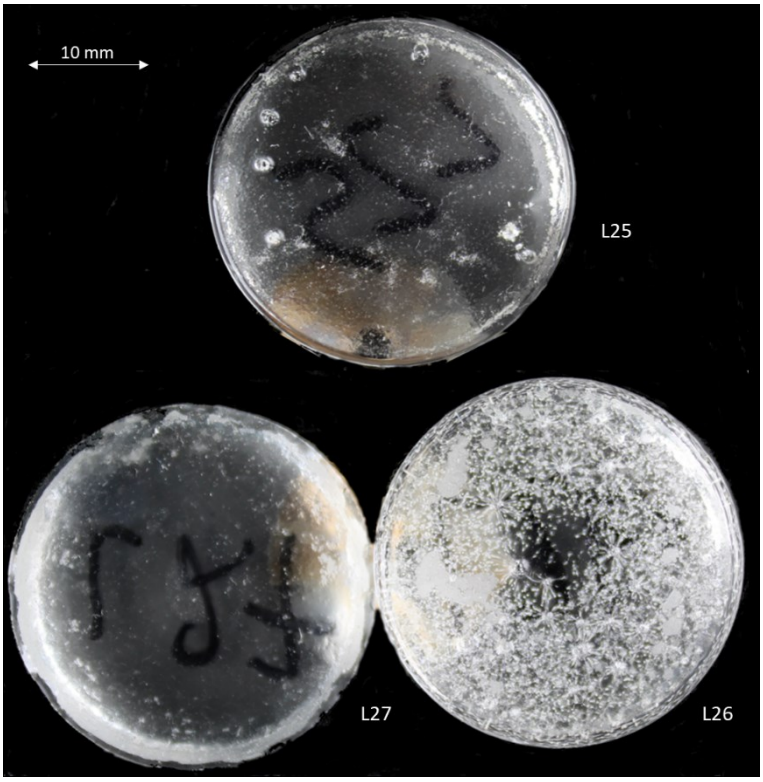

Figure 25 : L25 = Resin Pro (vacuum): L26 = Resin Pro (atmospheric pressure) and L27 = Struers (vacuum)

v. Test E

For this test all the elements were added: resin (Struers), black carbon (0.3 g), iodoform (10 wt%) and sample (3 g) containing a graphite concentrate. This test was pressurised only during curing time. Indeed, during previous work at ULiège, it had been shown that adding a pressure step during curing greatly reduced the volume of bubbles. In the same way that pressurisation produced better results than if the block was left in ambient air, it could be that pressurisation induces fewer bubbles and/or a weaker/non-existent exothermic reaction. The polished block (L74, Figure 26) shows a crackle which demonstrates clearly that an exothermic reaction has taken place when curing.

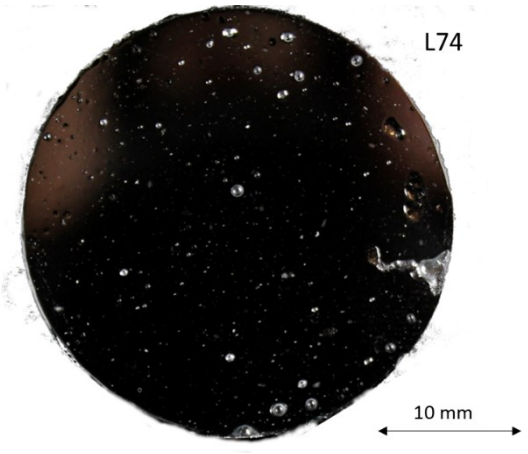

Figure 26: L74 – "Struers resin", black carbon (0.3 g), iodoform (10 wt%) and sample (3 g)

Then, to determine the origin of the exothermic reaction, it was first decided to test whether a resin-material mixture was the cause. To do this, a coarse sample was mixed with the resin (Struers). At the same time, other resins that had cured overnight were also subjected to this test to compare the results. The moulds were placed under vacuum during curing time. It seems to show a greater volume of bubbles than the tests without the added material (see Figure 27). The resin blocks made of "Resin Pro" and "Resion High" seem to have cured faster trapping more air bubbles than the other polished blocks.

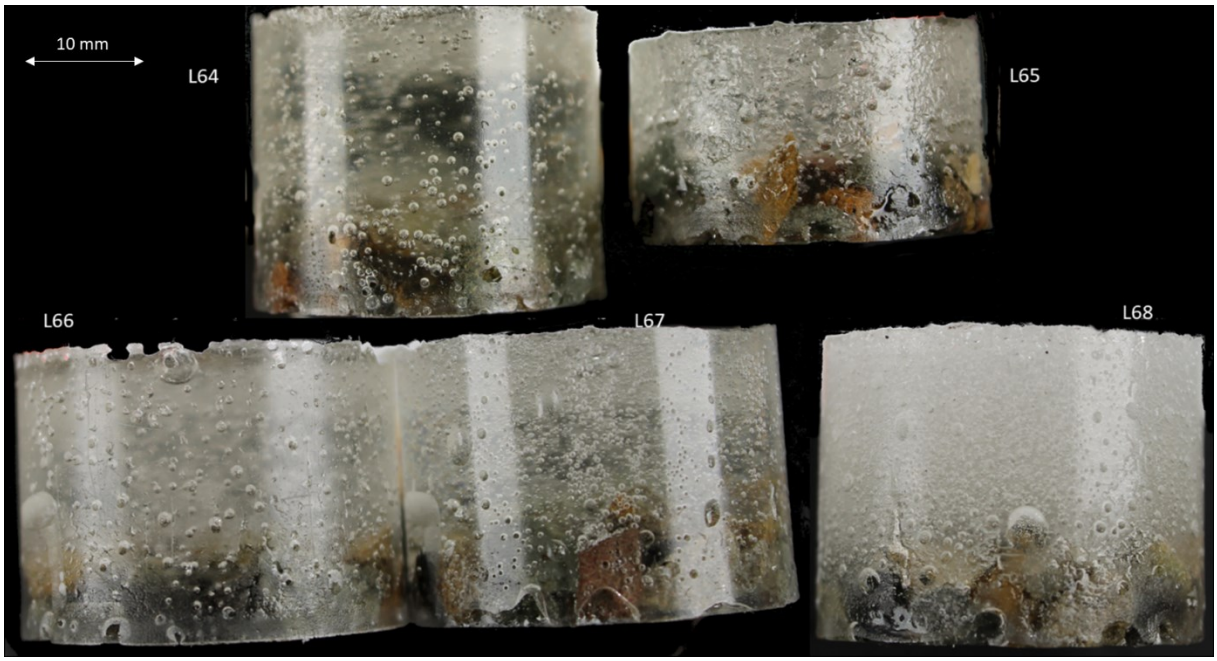

Figure 27 : L64 = Struers; L65 = Resin Pro; L66 = Resion Low; L67 = Resion Medium; L68 = Resion High

As no exothermic reaction was observed, it was wondered if the exothermic reaction with “Struers resin” was from the resin-iodoform mixture alone or if it was from the resin-BC-iodoform mixture. The curing of the polished blocks was carried out in the ambient air (atmospheric pressure) and under pressure (non-atmospheric, about 2.5 bars).

Figure 28 illustrates that even without BC, the “Struers resin” mixed alone with iodoform showed an exothermic reaction marked by the presence of large air bubbles. Moreover, it is more impressive in the atmospheric pressure suggesting that the higher pressure may limit this reaction.

Figure 28: L75 = Struers - iodoform -under pressure; L76 = Struers - iodoform – atmospheric pressure; L77 = Struers - iodoform - 0.1 g BC – under pressure; and L78 = Struers - iodoform - 0.1 g BC - atmospheric pressure

The test where all the elements were added (resin, hardener, black carbon (0.3 g), iodoform (10 wt%) and sample (3 g) containing a graphite concentrate was repeated using Resion Low as the resin to compare the two results together ("Struers resin" and "Resion Low"). "Resion Low" resin was chosen because of its short curing time (1 night). The addition of the sample makes it possible to see whether the contrast of the grey levels of the resin and the graphite under the SEM is good.

As can be seen in Figure 29, the resin blocks using "Resion Low" (L73) do not seem to show an exothermic reaction compared to "Struers resin" (L74), but only a large volume of air bubbles of varying sizes.

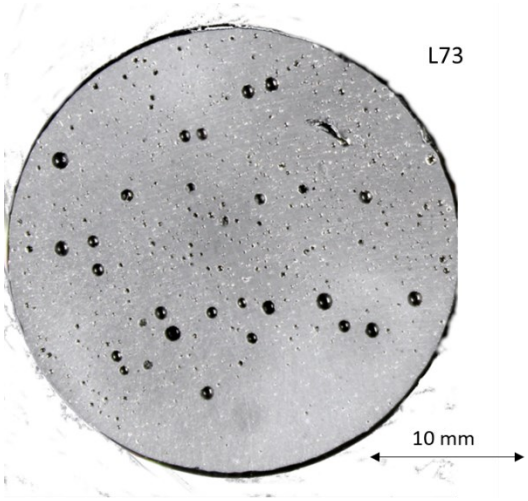

Figure 29: L73 – "Resion Low", black carbon (0.3 g), iodoform (10 wt%) and sample (3 g)

"Struers" resin induces an exothermic reaction in the resin-BC-iodoform mixture. However, "Resion Low" is not good enough in view of the large air bubbles present even with the effect of pressure. A polished block with "Resion High", iodoform (10 wt%) and a sample of pure graphite was made to examine whether the other extreme (Low vs High viscosity) of the "Resion" range has the same problem with air bubbles. Moreover, "Resion High" hardens faster than "Resion Low".

"Resion High" does not seem to be impacted by any reaction and the surface of examination is free of bubble (Figure 30). Also, reading under the SEM is feasible but the contrast could be improved by adding more iodoform. Therefore, the choice of 15 wt% as advised by Rahfeld & Gutzmer (2017) will be used thereafter.

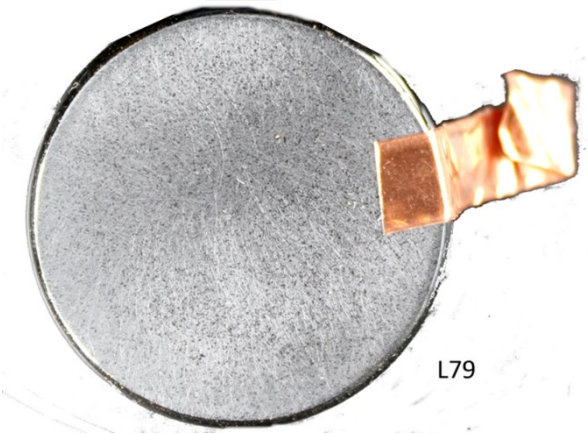

Figure 30: "Resion High" – iodoform – under pressure (polished block has been metalized)

Finally, a polished block, also cured under pressure, made of "Resion High" resin, iodoform, and BC (0.1 and 0.2 g) has been produced to ensure that no exothermic reaction would occur with the addition of BC. As shown in Figure 31, no reaction took place, and no bubbles were visible. In addition, the contrast under the SEM is excellent.

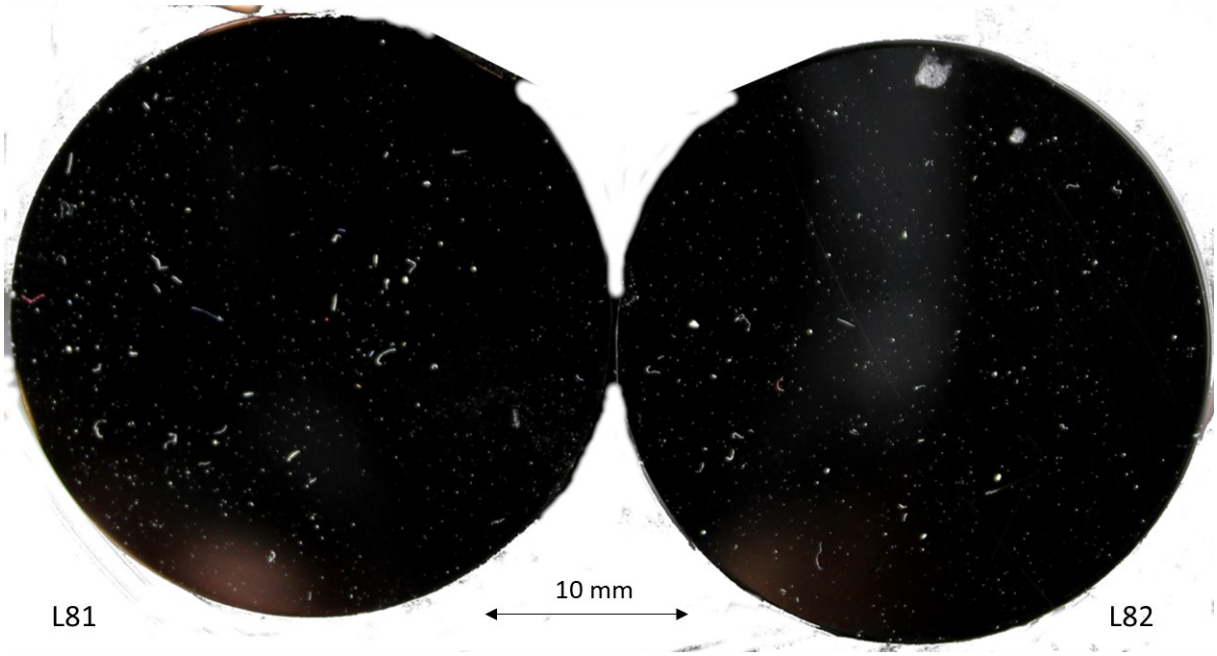

Figure 31 : L81 = "Resion High" - iodoform - 0.1g BC; and L82 = "Resion High" - iodoform (15 wt%) - 0.2g BC

Figure 32 below shows the correspondence between graphite observed (in brown) with an optical microscope and under the SEM (in black) on a polished block realised with the same procedure used as L81 and L82 (Figure 31) and the addition of a graphite concentrate. It shows the good contrast between the graphite, which is blacker, the resin, which is greyer, and the rest of the minerals, which are lighter than the resin.

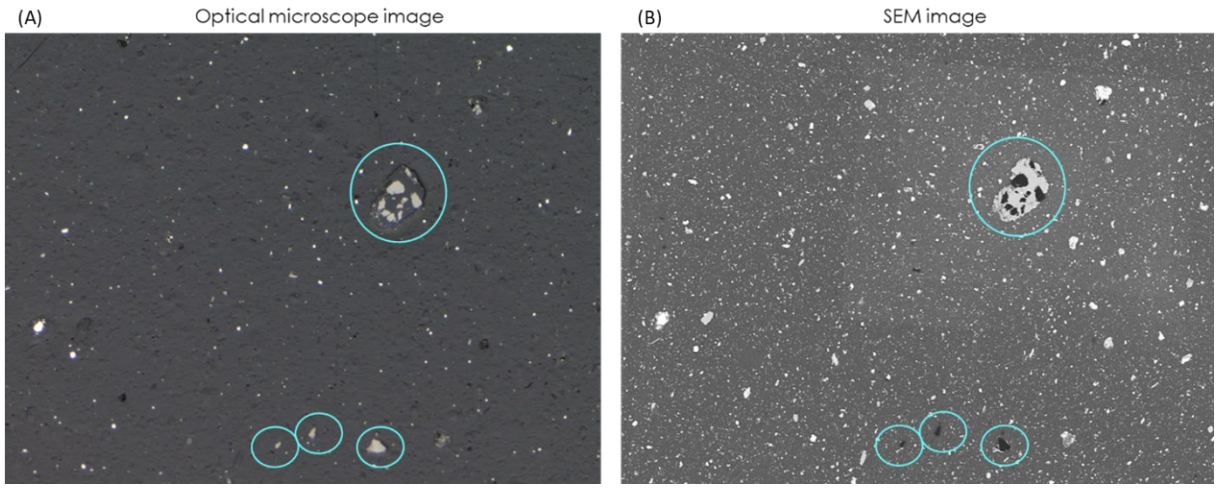

Figure 32: Correspondence between graphite particles observed in brown with an optical microscope (A) and under the SEM in black (B). The SEM image shows a good contrast between graphite, resin (grey) and other minerals (lighter particles)

In conclusion, "Resion High" can be used with BC and iodoform without risking having an exothermic reaction. In addition, pressurizing the material during curing prevents the formation of bubbles that can be seen macroscopically. It also seems that microscopically, the number of bubbles is greatly reduced so that one could almost say that there is none.

The diagram below (Figure 33) summarises the tests and their main results.

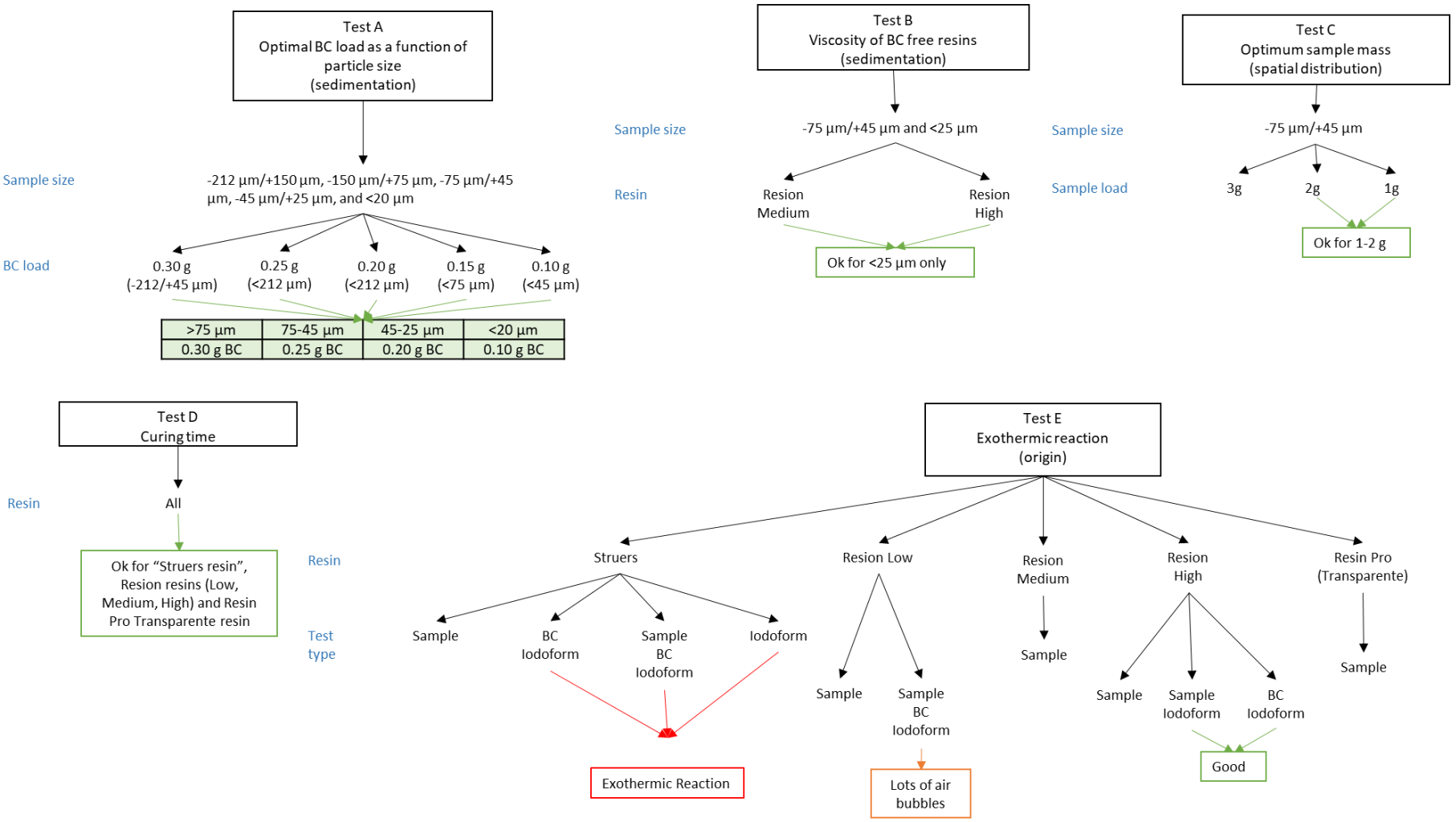

Figure 33: Summary of all tests conducted with their main results

5.2.4 Is it necessary to go through a vacuum step?

During these tests, an idea for improving the preparation also arose. As a reminder, in the recipe usually used at ULiège, after mixing the resin and BC, the mixture is degassed under vacuum. Then, once the sample and hardener had been added to the resin-BC mixture and placed in the mould, the whole is left to cure overnight under pressure (an addition from previous work at ULiège).

Still with the aim of eliminating as many air bubbles as possible, one method involved degassing after adding the BC to the resin before mixing for three hours, and then continuing with the usual vacuum degassing step.

The addition of this step showed no difference with the usual recipe. If going through the vacuum stage is not necessary, then it could be completely removed if the pressurisation stage during the curing time is used. A polished block was made using the usual preparation method, but with the removal of the vacuum degassing step after that the BC and resin had been mixed for three hours.

Figure 34 shows a portion of a block prepared without any vacuum degassing step. It can be seen that the block shows almost no bubbles, which is the same result as if the pressurisation step had been carried out during the curing time on a polished block following the original recipe used at Uliège. However, particles are stripped (black spots of various shapes) and this is due to the polishing process.

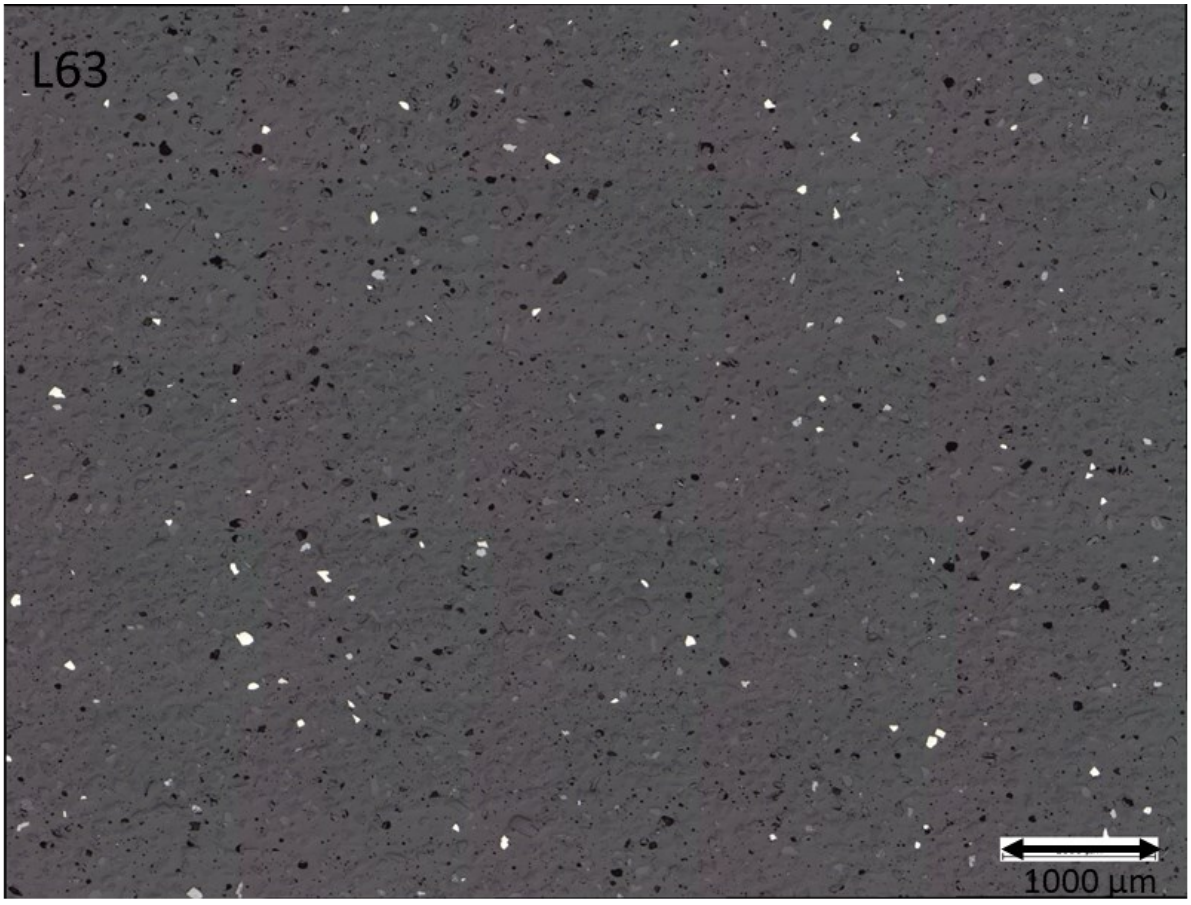

Figure 34: L63 = no step of vacuum, cured under pressure (with optical microscope)

As no major differences were observed, it was decided to eliminate the vacuum step and to keep only the pressurisation step as a means of degassing the resin block as it saves preparation time.

Below (Figure 35) is a schematic summary of the final preparation for a sample containing carbonaceous material, in this case native graphite, based on all the results.

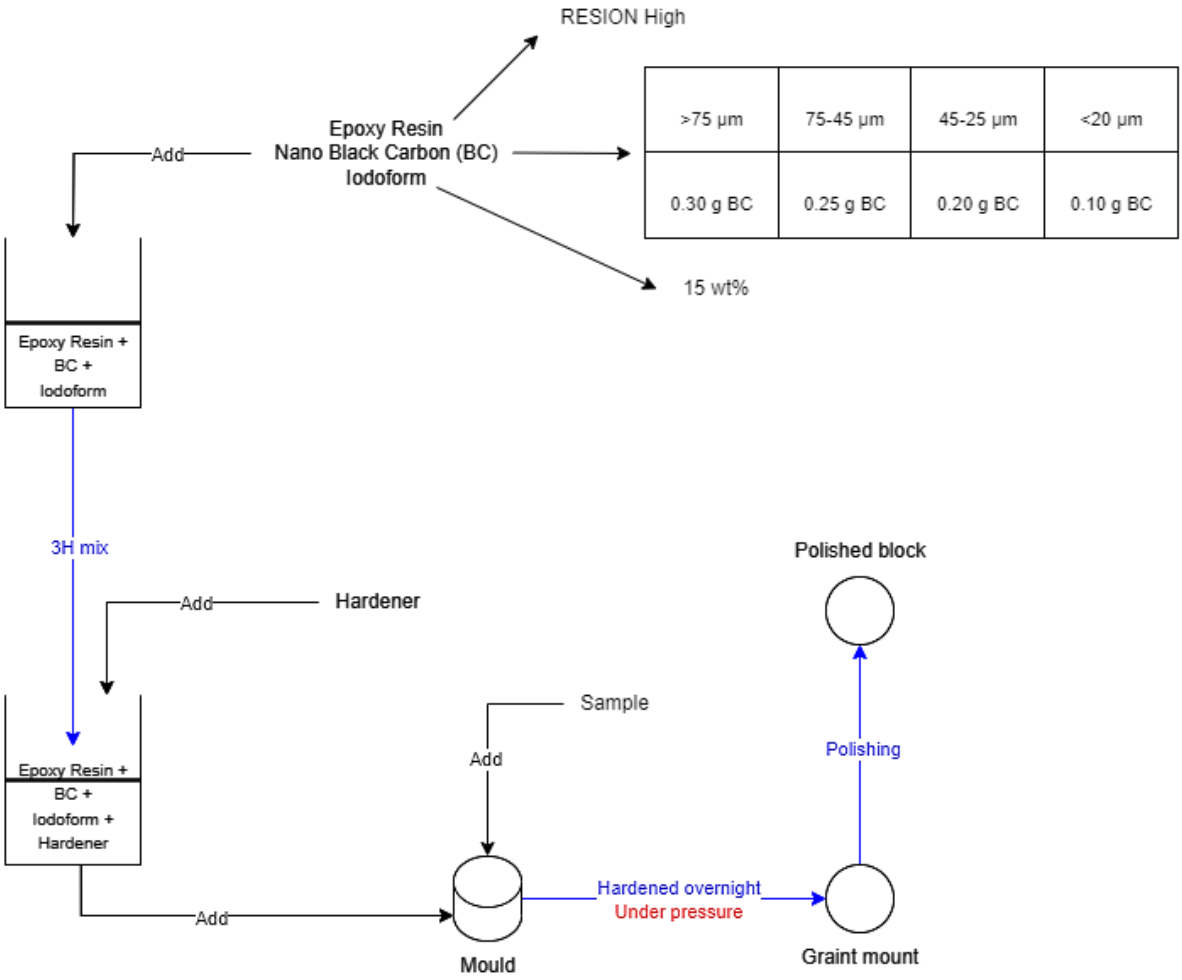

Figure 35: Schematic procedure for the final preparation of polished block

5.3 Results on SEM

Next, it is time to confirm whether the preparation gives satisfactory results when compared with the data from the chemical analyses.

As a reminder, three types of classification have been considered:

- The first classification deconvolved element C (carbon) from the spectrum, even though usually C is not, because if it were, it would "dilute" the wt% of the other elements due to the resin being rich in carbon and thus the stoichiometry of the mineral is further from the ideal one. This could make it difficult to differentiate between minerals with similar "diluted" stoichiometry.
- Another classification did not deconvolve C, which meant that the stoichiometry of the minerals was closer to the ideal one. To classify graphite, a limit on the grey level has been added so that each pixel with a level smaller than it, is classified as graphite.
- A final classification was to deconvolve the C and add a limit on the grey level for each mineral, i.e., graphite was below a said level and other minerals were above this level.

The first is to be avoided because the received signal sometimes contains elements other than C for a graphite particle. Indeed, to analyse graphite, which is composed of carbon, a light element, the voltage should be set lower than 20kV on the SEM (as set here for this project), but as all minerals need to be analysed this voltage is typically set to 20kV to be able to penetrate higher atomic number minerals such as sulphides. The electron beam therefore passes through the graphite and sometimes comes to analyse minerals lower down in the resin, which means that other elements than carbon are detected at a point where it should only be pure graphite. Figure 36 below, although produced using the third proposed classification, shows this variability in composition even though it is supposed to be pure graphite. As the latest classification takes account of the grey level, these analysis points with different compositions were well classified as graphite. However, using the first classification proposal, these analysis points were misclassified.

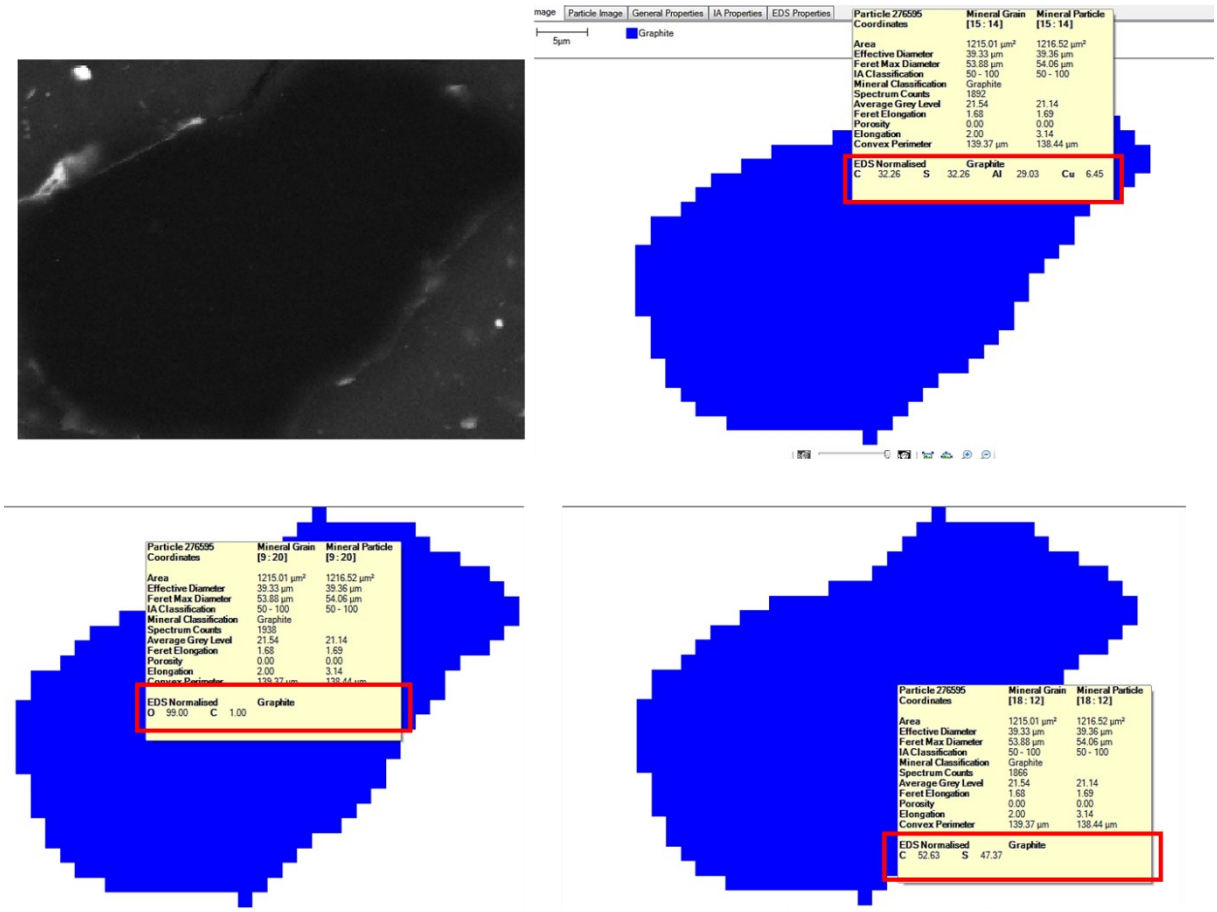

Figure 36: Graphite particle analysed using SEM by deconvolving C and taking into account the grey level. Different compositions at different analysis points, which could correspond to minerals other than graphite

The second classification, which does not recalculate the %C from the spectrum but takes account of the grey level, should also be avoided. Indeed, when an analysis point contained 100% C and the spectrum was deconvolved (without C), no other element was present. As a result, the point was recorded as “not analysed” by the software, even though a grey level corresponding to graphite had been recorded. These unanalysed points biased the liberation results.

The last classification method (deconvolving C and setting a grey level) is therefore the best classification to use, although the stoichiometry of the elements in the different minerals was not the ideal one, as seen in the previous Figure 36. Thus, for instance, for graphite, the percentage of C required was reduced and the grey level allowed a good classification. It was with the latter that the samples were finally analysed.

The graph below (Figure 37) shows the bulk mineralogy obtained. It can clearly be seen that the first 7 samples correspond to carbon concentrates (CC) and the last 7 to sulphide concentrates. In the first 7, the proportion of graphite, quartz, muscovite, and dolomite is higher than in the last 7, where the proportion of pyrite and arsenopyrite is much higher. As a result, the proportion of graphite, dolomite and silicate has decreased. It is also noted that sample G1078 (carbon concentrate) has a lower proportion of graphite compared to other carbon concentrates and, sample G1096 (sulphide concentrate) has a higher proportion of graphite than the other sulphide concentrates. However, these two samples are not related, i.e. they do not come from the same flotation series.

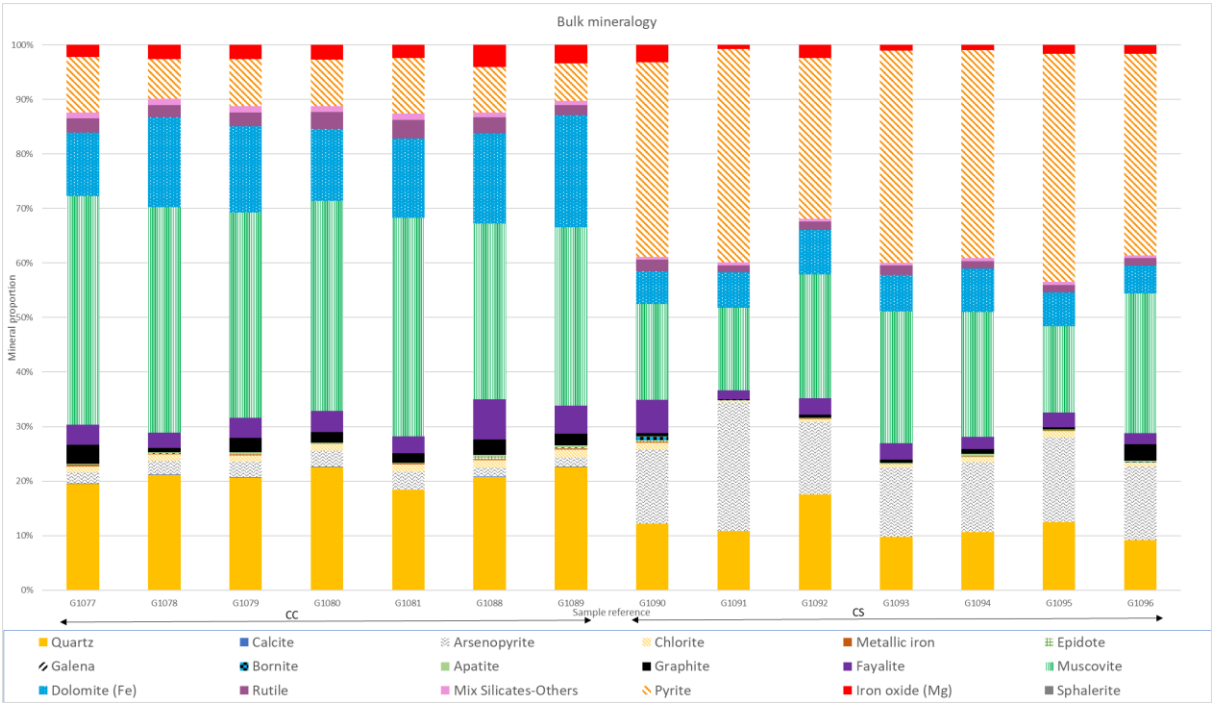

Figure 37: Bulk mineralogy of the samples

The graphs below (Figure 38) show the cumulative liberation of graphite in carbon concentrate (A) and sulphide concentrate (B). For the carbon concentrate, on average 70% of the graphite is liberated (average of all carbon concentrates) if it is considered that the particle is liberated when more than 80% of its surface is free. The last two samples of carbon concentrates (G1088 and G1089) have the most graphite liberated while G1077, G1079 and G1080 appear to be the samples with the lowest proportion of graphite liberated. On average (average of all sulphides concentrates), about 58% of the graphite is liberated in sulphides concentrate. The last concentrate, G1096, has a different trend than the others, as can be seen. The average rises to 67% if it is considered an “outlier”. G1090 and G1091 are the samples with the most graphite liberated while G1092, G1093 and G1096 appear to be the samples with the lowest proportion of graphite liberated.

These two averages (concerning liberation) show that much of the graphite was "associated" with the resin in the polished block. Regarding associations with other minerals, using SEM results, graphite was found to be mainly associated with quartz, followed by dolomite and fayalite for carbon concentrates. For sulphide concentrates, graphite is mainly associated with pyrite, followed by quartz and dolomite.

A large proportion of the graphite in the sulphide concentrates is free, and so should not have floated. It is therefore assumed that graphite was collected in the final concentrate due to entrainment by the flow.

(A)

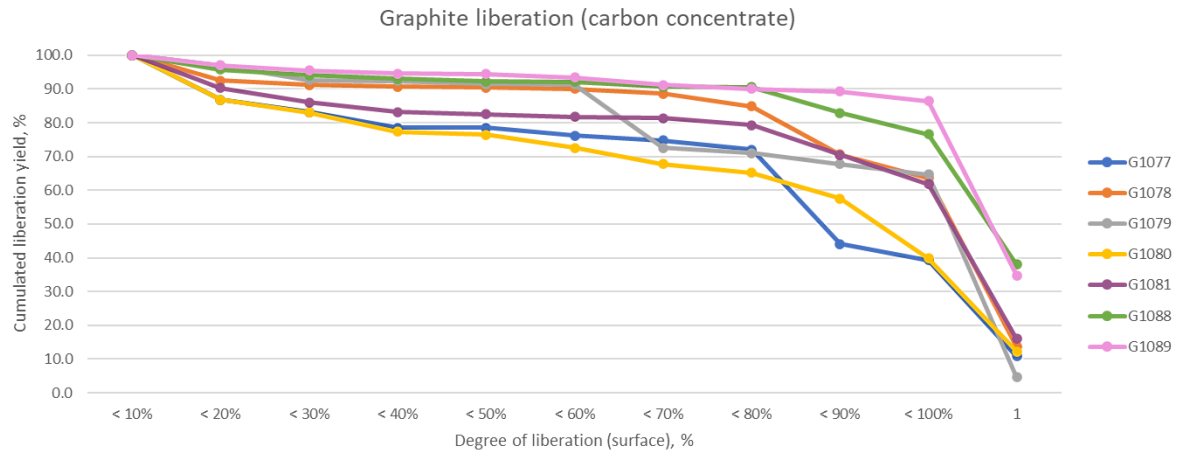

(B)

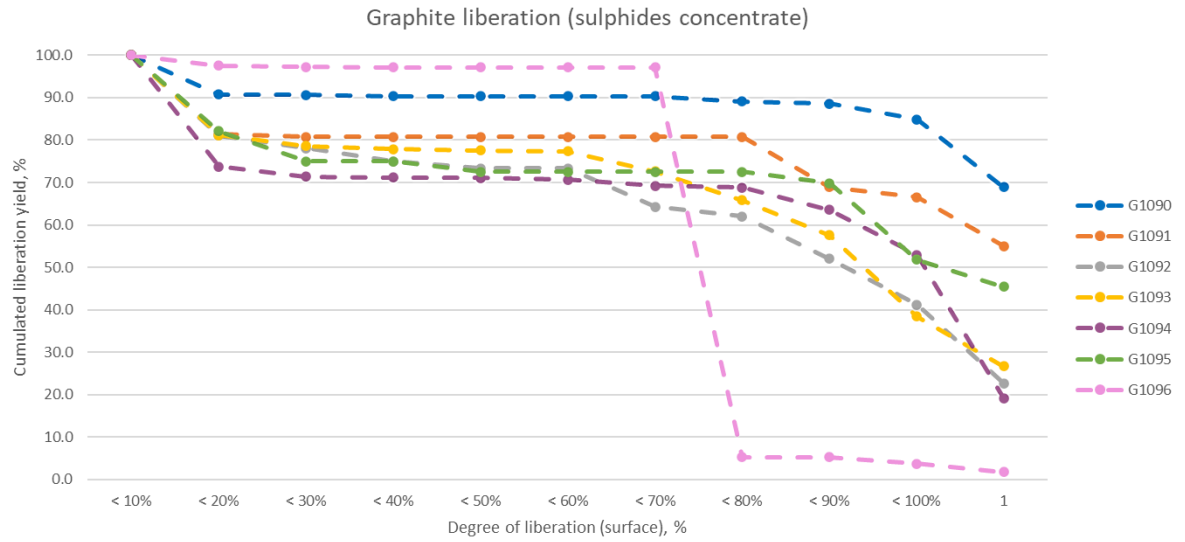

Figure 38: Cumulated liberation of carbon concentrate (A) and sulphides concentrate (B) in relation to their degree of liberation

The total percentage of C and S (%C tot and %S tot) was recalculated from the minerals carrying these two elements (Table 5 and Table 6). The results (Table 7) were then compared with the data obtained from the chemical analyses.

Table 5: Carbon source

Mineral	wt% C
Calcite	12
Graphite	1
Dolomite	13.03

Table 6: Sulfur source

Mineral	wt% S
Arsenopyrite	19.69
Galene	13.4
Bornite	25.56
Pyrite	53.45
Sphalerite	33.06

Table 7: %S and %C from chemical analyses and recalculated from SEM bulk mineralogy results

Sample	*Type*	*%S TOT (Chem.)*	*%S TOT (MEB)*	*%C TOT (Chem.)*	*%C TOT (MEB)*
G1077	CC	4	5.9	14.6	5.0
G1078	CC	3.2	4.4	11.8	2.9
G1079	CC	3.6	5.2	12.4	4.6
G1080	CC	3.7	5.1	11.1	3.6
G1081	CC	4.6	6.1	12.7	3.6
G1088	CC	3.4	4.8	10.3	5.0
G1089	CC	2.5	4.0	9.2	4.8
G1090	CS	23.5	21.9	3.1	1.4
G1091	CS	21.1	25.6	3.2	1.0
G1092	CS	20.6	18.3	3.3	1.6
G1093	CS	26.1	23.3	2.4	1.4
G1094	CS	20.5	22.9	2.7	1.9
G1095	CS	21.9	25.4	2.7	1.2
G1096	CS	20.9	22.4	3.3	3.7

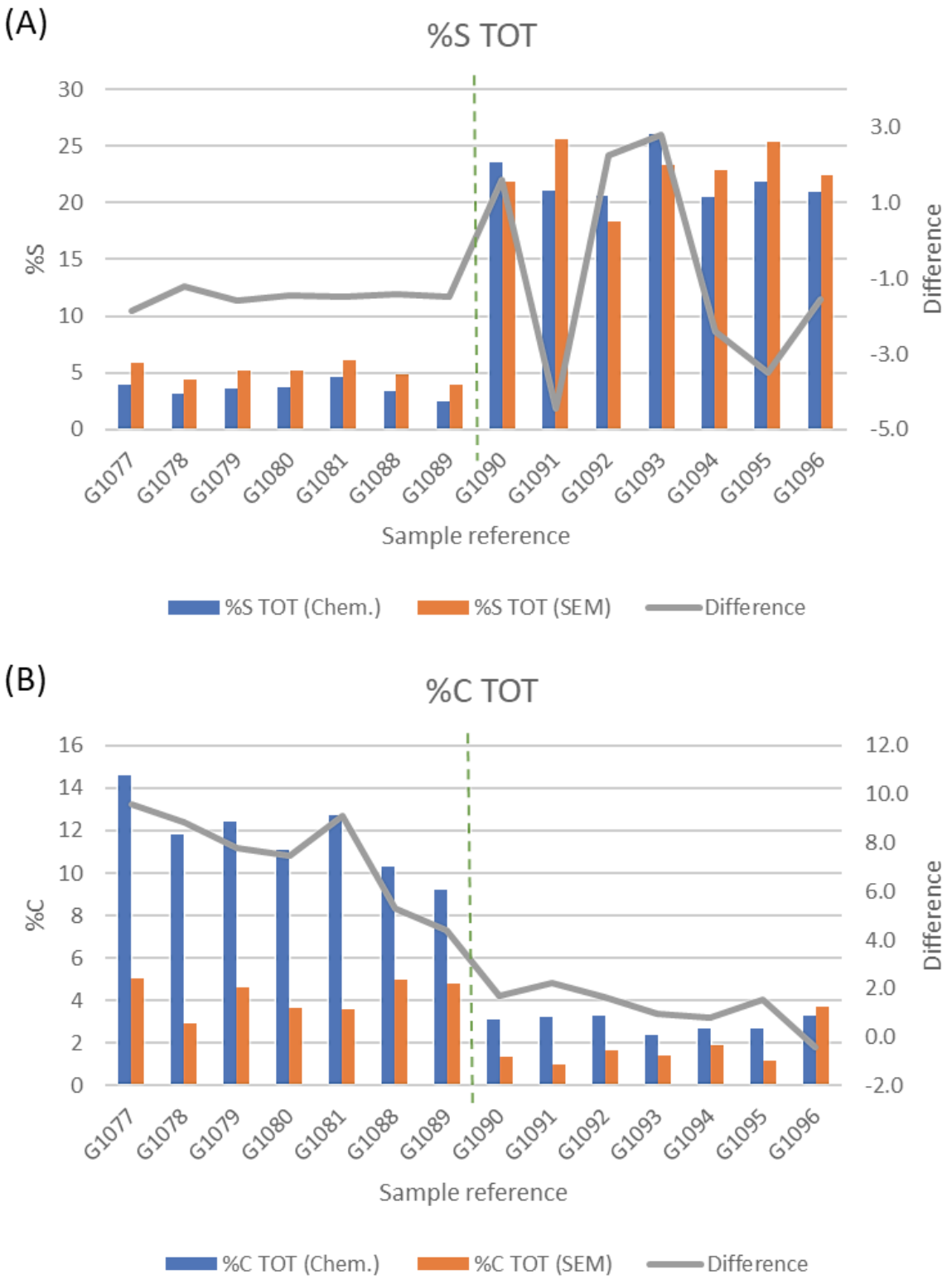

Figure 39: Graphs illustrating %S tot (A) and %C tot (B) from chemical analyses and recalculated from SEM bulk mineralogy results as well as their difference

The %S tot calculated from the SEM results shows that, in general, the SEM overestimated the results (compared with the chemical analysis values). The values are nevertheless fairly close to each other. A

certain trend can be seen for CC (samples G1077 to G1089), with values overestimated by more or less 1.5% (as seen in Figure 39). Whereas the CS values are sometimes overestimated and sometimes underestimated, and the variation in relation to the chemical analysis data is greater. But the values are also higher (around 22% of S tot in the CS), so proportionally speaking the values are within the same range. When it comes to C% tot, it is a completely different story. It is generally underestimated, and this underestimation is much more marked in CC (two to three times lower). This means that a large proportion of the carbon source has not been analysed.

Different hypotheses have been put forward regarding this loss:

- Do the particles smaller than 7 µm count for the most carbon source minerals?
- Is it a loss linked to the boundary of graphite with other minerals and therefore particles with a lighter grey level so that the average grey level of this boundary is higher than the threshold applied to classify graphite? But graphite is also "gained" due to the relief at the edge of the particle which has not been removed even with the size limitation, and graphite is also “gained” with stripped particles that have the same grey level as graphite.
- Are carbon containing minerals not analysed by the SEM due to poor polishing (not selected by the software as a particle)?
- Is there another type of carbon source that cannot be detected with the SEM?

The most likely hypothesis would be the first. As a reminder, a limitation was imposed on the size to avoid analysing the relief which has the same level of grey in the backscattered electron image (any particles smaller than 7 µm was not analysed by the SEM). To determine the proportion of carbon below 7 µm, a new analysis was carried out on G1077 alone to obtain the bulk mineralogy of particles below this size. In this way, it is possible to compute the proportion of carbon above and below 7 µm so that the total C% value corresponds as closely as possible to the chemical analysis value. Then, using the two newly obtained proportions, the rest of the data could be weighted to obtain valid results. It is also expected that for the cumulative liberation graphs, the curves "rise", i.e., more graphite would be liberated. Indeed, a certain proportion of graphite, of smaller size, and therefore more liberated, would be added (a more ground material is expected to be more liberated).

Calculated from the SEM data, the total C% is 18.22 and the total S% is 8.38 for the portion below 7µm. With these two values, no value can be assigned as to the proportion that the 7µm represents to obtain values close to those obtained by chemical analyses.

This raises the question of the validity of the SEM results. Is it the preparation that poses the problem? If one goes through the preparation of the polished blocks again:

- Is it a homogenisation problem? It should not as the samples were homogenised before a certain quantity was taken for the polished blocks. Furthermore, these were in a cylinder vial, so the mass of the sample required for a polished block was taken from the top. As graphite is light, if the sample had not been homogenised properly, it would have had to be taken in larger quantities as most of the graphite grains would have been contained in the top of the tube which is not the case.
- Is this a question of sedimentation during the curing process? According to the tests carried out, the preparation should not sediment.
- Is there a problem with the way the sample is mixed with the resin? For these polished blocks, mixing was carried out mechanically. Therefore, this should not be the cause.
- Is it poor contrast? The tests also showed that the contrast was good. If graphite is present, the software should have seen it in the BSE image.

Since the preparation should not be the cause, is it possible that it is the sample itself that is causing the problem? Since graphite is a soft mineral and easy to cut due to its excellent cleavage, is it possible that a large proportion of the graphite is at a smaller particle size and that, with the magnification chosen for the analyses, the particles were not "seen" by the software? For instance, if one considers that the analysis above 7µm is valid and that it is the analysis below 7µm that poses a problem due to this assumption, to best fit the chemical analyses values and considering that the portion of %C less than 7µm is equivalent to 70% of the total wt% C of the sample, the wt% of the graphite should be 20 times greater than that obtained.

6 Suggested improvements

As mentioned before, there is a stripping problem. This one seems to particularly affect the fine grains. Indeed, the smaller they are, the less surface adheres to the resin and with the pressure applied by the polishing machine they are stripped off. Moreover, these stripped particles also appear with the same level of grey as graphite when the polished block is prepared with iodoform (Figure 40). To try solving this problem, some tests began with manual polishing on the roughest discs so that the minimum pressure applied was lower than that of the polishing machine (which cannot go below five Newtons). The polishing was then resumed on the finest discs, such as MD piano 2000 and then the rest of the discs with the polishing machine. There has been an improvement, but fine particles are still frequently stripped off. Moreover, as discussed in a previous section, there is a relief problem that could also be resolved with better polishing. It is therefore suggested that further work have to be considered on polishing methods to solve these problems.

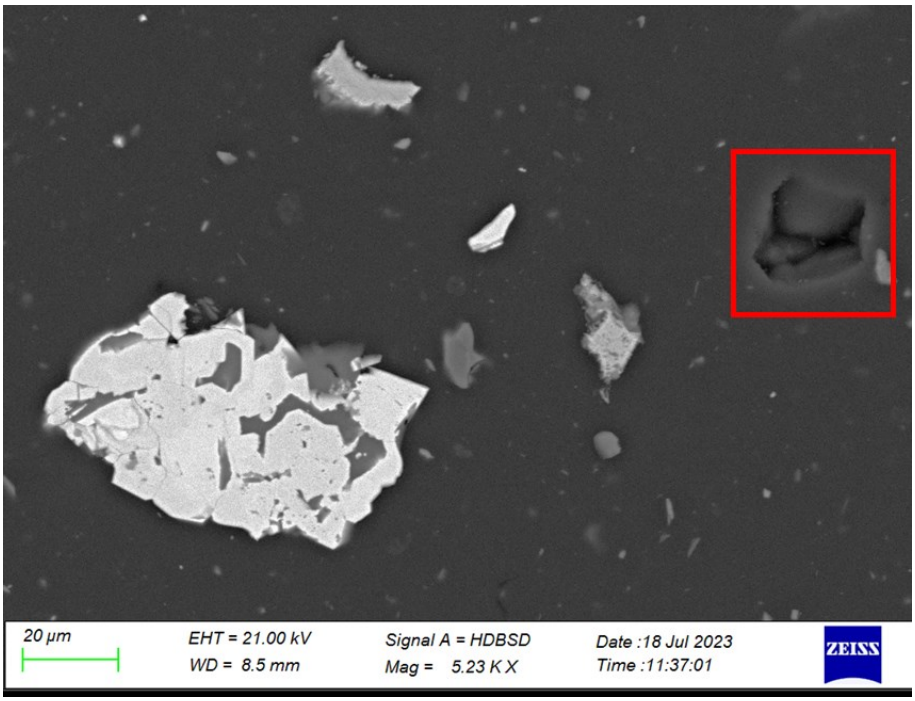

Figure 40: Stripped particle appearing in black (framed in red) when prepared according to the new protocol (Resion High-iodoform-BC)

7 Another application for the protocol: black mass?

Black mass is the term used to describe the powdery concentrate of active battery materials (such as lithium-ion) resulting from pre-treatment, including crushing and shredding. The powder therefore contains the transition metal oxides originally present in the battery (Ni, Co and/or Mn, iron phosphate, etc) as well as Li for the cathode part, graphite that is partially still lithiated (mainly used at the moment) for the anode part as well as the fraction of black carbon used at both the anode and cathode for electronic conductivity. However, due to the intrinsic imperfection of the thermo-mechanical pre-treatment, electrode metals (Al and Cu), polymers and traces of residual electrolyte may contaminate this concentrate.

There is currently a desire to develop the recycling of these batteries as global demand for battery manufacturing increases, and to achieve a more circular economy, especially as some of the materials that make up batteries and that can be extracted from them are considered critical. Recycling black mass is therefore important to supplement and/or reduce the supply of virgin materials and, at the same time, reduce the carbon footprint of the battery supply chain (particularly linked to mining activity). Hence, environmentally sustainable and economically viable recycling technologies are becoming a key area of focus.

The development of these new recycling technologies therefore involves characterising the samples produced, and this could be done using SEM to quantify the minerals/materials present and their associations. With the development of this protocol, the graphite in batteries may now also be properly characterised allowing recycling processes to be adapted to extract the desired materials.

8 Conclusions

The aim of this project was to develop a methodology for characterising native graphite in gold ore using an automated mineralogy system. The preparation of polished blocks which is the support allowing good characterisation, developed within this framework proved to be satisfactory for the analysis of graphite by SEM. The fact that the proposed preparation is an adaptation of the method usually used at the University of Liège - itself based on the method of Bouzahzah *et al.* (2015) - avoids the recurrent problems of sample preparation as polished blocks (differential sedimentation of the particles, touching particles and systematic orientation of the particles). Moreover, adjusting the black carbon load according to the particle size of the sample not only avoids the supply of air contained in the BC aggregates which create air bubble, but also saves material. Using the “Resion High” resin and letting the polished block cure under 2.5 bar pressure made it possible to no longer face the exothermic reaction when the iodoform - which, as a reminder, is necessary to obtain good contrast in the backscattered electron image - is added to the mixture. This absence of exothermic reaction not only allows easier polishing than if the block had reacted, but also to limit the presence of air bubbles which can be confused by the software as being graphite due to the same level of grey in backscattered electron image.

However, the polishing of resin blocks needs to be improved in order to obtain more accurate results by avoiding the stripping of the particles and the formation of relief on the edges of the particles, which both can also be confused by the software as being graphite due to the same level of grey in backscattered electron image. This would also make it possible to lift the limitation on the size that was imposed in this work, and which subsequently created some difficulties in the analysis of the results.

It is finally deemed that the proposed classification for the Mineralogic software, based on chemical composition and grey level with double thresholding, allows good classification of minerals and therefore good characterisation with the proposed preparation for polished block of this document.

That being said, to fully confirm the hypothesis that the graphite particles were too small to be seen at the magnification used for this study, it would have been necessary either to repeat the analysis at a higher magnification, but this would increase the acquisition time, or it would have been necessary to split the sample into sub-samples according to size and to conduct chemical analyses on each fraction to determine its composition. This would have revealed whether most of the carbon was in a smaller fraction or not.

9 References

Ali, A. S. (2020). Application of nanomaterials in environmental improvement. In M. Sen (Ed.), *Nanotechnology and the Environment* (p. 20). IntechOpen. doi:http://dx.doi.org/10.5772/intechopen.91438

Bouzahzah, H. (2013). *Modification et amélioration des tests statiques et cinétiques pour une prédiction fiable du drainage minier acide.* PhD Thesis, Université du Québec en Abitibi-Témiscamingue (UQAT), Rouyn-Noranda, Québec-Canada.

Bouzahzah, H., Benzaazoua, M., Mermillod-Blondin, R., & Pirard, E. (2015). A novel procedure for polished section preparation for automated mineralogy avoiding internal particle settlement. *12th International Congress for Applied Mineralogy (ICAM).* Istanbul, Turkey.

Butcher, A. (2010). practical guide to some aspects of mineralogy that affect flotation. In C. J. Greet (Ed.), *Flotation plant optimisation : a metallurgical guide to identifying and solving problems in flotation plants* (pp. 83-94). Carlton, Victoria: AusIMM.

Creelman, R. A., & Ward, C. R. (1996). A scanning electron microscope method for automated, quantitative analysis of mineral matter in coal. *International Journal of Coal Geology, 30*(3), 249-269. doi:https://doi.org/10.1016/0166-5162(95)00043-7

Dimov, S. S., & Hart, B. (2016). Study on surfactants for passivation of naturally occuring carbonaceous matter in gold bearing ores. *XXVIII International Mineral Processing Congress Proceedings* (p. 11). Québec city, Canada: Canadian Institute of Mining, Metallurgy and Petroleum.

Donskoi, E., Raynlyn, T. D., & Poliakov, A. (2018). Image analysis estimation of iron ore particle segregation in epoxy blocks. *Minerals Engineering, 120*, 102-109. doi:https://doi.org/10.1016/j.mineng.2018.02.024

Gomez, C. O., Strickler, D. W., & Austin, L. G. (1984). An iodized mounting medium for coal particles. *Journal of Electron Microscopy Technique, 1*(3), 285-287. doi:https://doi.org/10.1002/jemt.1060010307

Goodall, W. R., Leatham, J. D., & Scales, P. J. (2005). A new method for determination of preg-robbing in gold ores. *Minerals engineering, 18*(12), 1135-1141. doi:https://doi.org/10.1016/j.mineng.2005.05.014

Graham, S. D., Brough, C., & Cropp, A. (2015). An introduction to ZEISS mineralogic mining and the correlation of light microscopy with automated mineralogy: A case study using BMS and PGM analysis of samples from a PGE-bearing chromite prospect. *Proceedings of the Precious Metals 2015*, (p. 11). UK.

Grant, D. C., Goudie, D. J., Shaffer, M., & Sylvester, P. (2016). A single-step trans-vertical epoxy preparation method for maximising throughput of iron-ore samples via SEM-MLA analysis. *Applied Earth Science, 125*(1), 57-62. doi:https://doi.org/10.1080/03717453.2015.1104056

Guay, W. J. (1981). The treatment of refractory gold ores containing carbonaceous material and sulfides. *Paper presented at the 110th AIME Meeting on Gold and Silver-leaching.* Chicago, Illinois.

Hart, B. R., Dimov, S. S., Mermillod-Blondin, R., & Fournier, J. (2011). Procedure for characterization of carbonaceous matter in an ore sample with estimation towards its preg-robbing capacity.

World Gold conference, (pp. 35-50). Montreal, QC, Canada. Retrieved February 28, 2023, from https://www.911metallurgist.com/wp-content/uploads/2016/10/PREG-ROBBING-CAPACITY.pdf

Helm, M., Vaughan, J., Staunton, W. P., & Avraamides, J. (2009). An investigation of the carbonaceous component of preg-robbing gold ores. *World gold conference*, (pp. 139-144). Johannesburg, South Africa. Retrieved February 28, 2023, from https://d1wqtxts1xzle7.cloudfront.net/35065941/An_Investigation_of_the_Carbonaceous_Component_of_Preg-robbing_Gold_Ores-libre.pdf?1412889777=&response-content-disposition=inline%3B+filename%3DAn_investigation_of_the_carbonaceous_com.pdf&Expires=1677598001

Hiemstra, S. A. (1985). The Role of Applied Mineralogy in Ore Beneficiation as Illustrated by Case Histories. *2nd International Congress on Applied Mineralogy in the Minerals Industry*, (pp. 9-20). Los Angeles, California, USA.

Jackson, B. R., Reid, A. F., & Wittenberg, J. C. (1984). *Rapid production of high quality polished sections for automated image analysis of minerals.* Technical note.

Kwitko-Ribeiro, R. (2012). New sample preparation developments to minimize mineral segregation in process mineralogy. In M. Broekmans (Ed.), *Proceedings of the 10th International Congress for Applied Mineralogy (ICAM)*, (pp. 411-417). Trondheim, Norway. doi:https://doi.org/10.1007/978-3-642-27682-8_49

Marsden, J. O., & House, C. L. (2006). *The chemistry of gold extraction* (2nd ed.). Littleton, Colorado, USA: Society for Mining, Metallurgy, and Exploration, Inc. (SME).

Mollenhauer, H. (1993). Artifacts caused by dehydration and epoxy embedding in transmission electron microscopy. *Microscopy research and technique, 26*(6), 496-512. doi:https://doi.org/10.1002/jemt.1070260604

Ng, W. S., Wang, Q., & Chen, M. (2022). A review of Preg-robbing and the impact of chloride ions in the pressure oxidation of double refractory ores. *Mineral Processing and Extractive Metallurgy Review, 43*(1), 69-96. doi:https://doi.org/10.1080/08827508.2020.1793142

O'Brien, G., Gu, Y., Adair, B. J., & Firth, B. (2011). The use of optical reflected light and SEM imaging systems to provide quantitative coal characterisation. *Minerals Engineering, 24*(12), 1299-1304. doi:https://doi.org/10.1016/j.mineng.2011.04.024

Ofori-Sarpong, G., Tien, M., & Osseo-Asare, K. (2010). Myco-hydrometallurgy: Coal model for potential reduction of preg-robbing capacity of carbonaceous gold ores using the fungus, Phanerochaete chrysosporium. *Hydrometallurgy, 102*(1-4), 66-72. doi:https://doi.org/10.1016/j.hydromet.2010.02.007

Osseo-Asare, K. A., Afenya, P. M., & Abotsi, G. M. (1984). Cabonaceous matter in gold ores: isolation, characterization and adsorption behaviour in aurocyanide solutions. In V. Kudryk, D. A. Corrigan, & W. W. Liang (Eds.), *Precious Metals: Mining, Extraction and Processing* (pp. 125-144). New York: Metallurgical Society of AIME.

Pyke, B. L., Johnston, R. F., & Brooks, P. (1999). The characterisation and behaviour of carbonaceous material in a refractory gold bearing ore. *Minerals Engineering, 12*(8), 851-862. doi:https://doi.org/10.1016/S0892-6875(99)00073-4

Radtke, A. S., & Scheiner, B. J. (1970). Studies of hydrothermal gold deposition (I). Carlin gold deposit, nevada, the role of carbonaceous materials in gold deposition. *Economic Geology, 65*(2), 87-102. doi:https://doi.org/10.2113/gsecongeo.65.2.87

Rahfeld, A., & Gutzmer, J. (2017). MLA-based detection of organic matter with iodized epoxy resin—An alternative to Carnauba. *Journal of Minerals and Materials Characterization and Engineering, 5*(4), 198-208. doi:https://doi.org/10.4236/jmmce.2017.54017

Raja, P. M., & Barron, A. R. (2023). 1.10: Total Carbon Analysis. In P. M. Raja, & A. R. Barron, *Physical Methods in Chemistry and Nano Science* (pp. 1.10.1-1.10.6). LibreTexts. Retrieved 06 12, 2023, from LibreTexts Chemistry: https://chem.libretexts.org/Bookshelves/Analytical_Chemistry/Physical_Methods_in_Chemistry_and_Nano_Science_(Barron)/01%3A_Elemental_Analysis/1.10%3A_Total_Carbon_Analysis

Rees, K. L., & Van Deventer, J. S. (2000). Preg-robbing phenomena in the cyanidation of sulphide gold ores. *Hydrometallurgy, 58*(1), 61-80. doi:https://doi.org/10.1016/S0304-386X(00)00131-6

Røisi, I., & Aasly, K. (2018). The effect of graphite filler in sample preparation for automated mineralogy–a preliminary study. *Mineralproduksjon, 8*, A1-A23. Retrieved 05 04, 2023, from http://mineralproduksjon.no/wp-content/uploads/2018/06/MP8-VA-R%C3%B8isi-PRINT2.pdf

Sandmann, D. (2015). *Method development in automated mineralogy.* [PhD Thesis], TU Bergakademie, Freiberg. Retrieved 05 04, 2023, from https://tubaf.qucosa.de/api/qucosa%3A23008/attachment/ATT-0/

Shaffer, M. (2009). Sample preparation methods for imaging analysis. *Geometallurgy and Appl. Mineralogy 2009, Conference of Mineralogists.*

Smythe, D. M., Lombard, A., & Coetzee, L. L. (2013). Rare earth element deportment studies utilising QEMSCAN technology. *Minerals Engineering, 52*, 52-61. doi:https://doi.org/10.1016/j.mineng.2013.03.010

Stenebråten, J. F., Johnson, W. P., & Brosnahan, D. R. (1999). Characterization of Goldstrike ore carbonaceous material: Part 1: Chemical characteristics. *Mining, Metallurgy & Exploration, 16*, 37-43. doi:https://doi.org/10.1007/BF03402817

Stenebråten, J. F., Johnson, W. P., & McMullen, J. (2000). Characterization of Goldstrike ore carbonaceous material. Part 2: Physical characteristics. *Minerals and Metallurgical Processing, 17*(1), 7–15. doi:https://doi.org/10.1007/BF03402823

Sylvester, P. J. (2012). Chapter 1: Use of the mineral liberation analyzer (MLA) for mineralogical studies of sediments and sedimentary rocks. In R. Raeside (Ed.), *Quantitative Mineralogy and Microanalysis of Sediments and Sedimentary Rocks* (Vol. 42, pp. 1-16). St. John's, Newfoundland and Labrador, Canada. Retrieved 05 03, 2023, from https://d1wqtxts1xzle7.cloudfront.net/51192570/CHAPTER_1-_USE_OF_THE_MINERAL_LIBERATION_ANALYZER-libre.pdf?1483583392=&response-content-disposition=inline%3B+filename%3DUSE_OF_THE_MINERAL_LIBERATION_ANALYZER_M.pdf&Expires=1683125100&Signature=ViIubLMotSP1

Ul-Hamid, A. (2018). Contrast Formation in the SEM. In A. Ul-Hamid, *A Beginners' Guide to Scanning Electron Microscopy* (pp. 77-128). Dhahran, Saudi Arabia: Springer. doi:https://doi.org/10.1007/978-3-319-98482-7

Van den Berg, R. (2000). *Inhibition of the pregrobbing phenomenon in gold ores.* Master thesis, Cape Technikon, Cape Town, Afrique du Sud. Retrieved February 21, 2023, from https://core.ac.uk/download/pdf/148364834.pdf

Van Vuuren, C. P., Snyman, C. P., & Boshoff, A. J. (2000). Gold losses from cyanide solutions part II: The influence of the carbonaceous materials present in the shale material. *Minerals engineering, 13*(10-11), 1177-1181. doi:https://doi.org/10.1016/S0892-6875(00)00100-X